Laboratori Nazionali del Gran Sasso

Le frontiere e i confini della scienza

Il Metodo Scientifico nelle Scienze della Natura. Un'applicazione alla Fisiologia

SCOPERTA E RISCOPERTA DELLA ECCITABILITA' ELETTRICA ANIMALE

Massimiliano Zaniboni
(Dipartimento di Bioscienze, Università degli Studi di Parma)

Luigi Galvani (1737-1798)

“vis electrica” interna

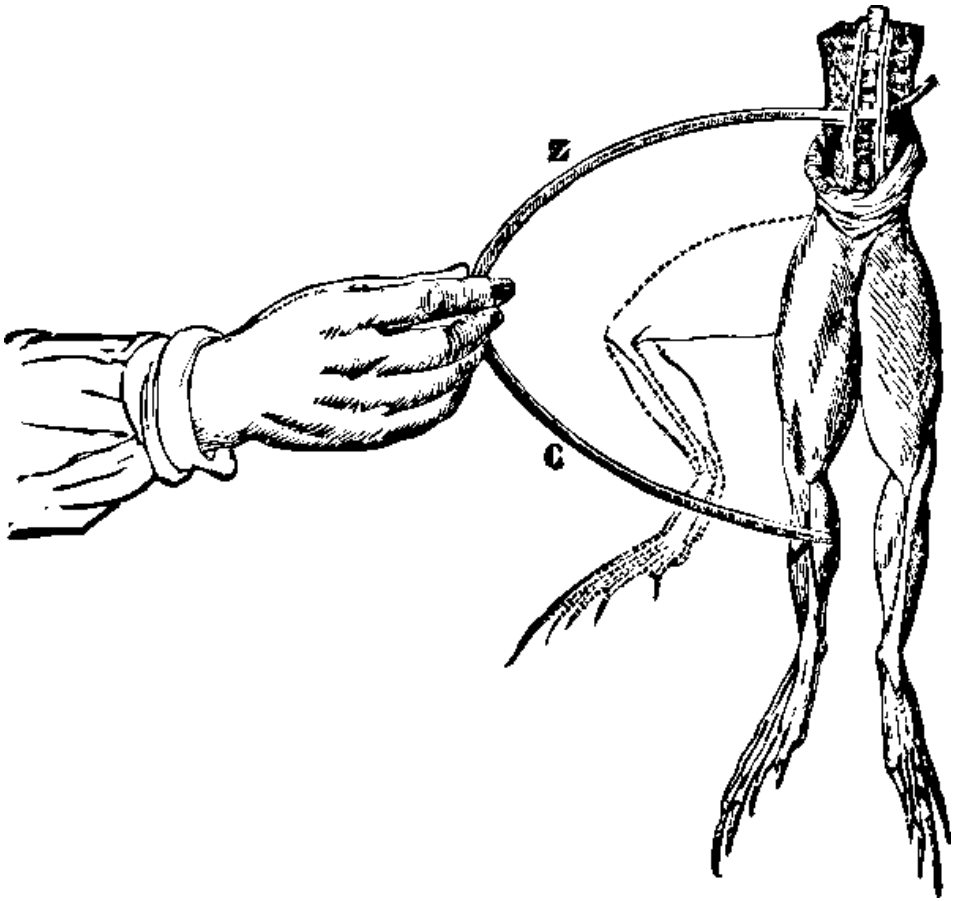

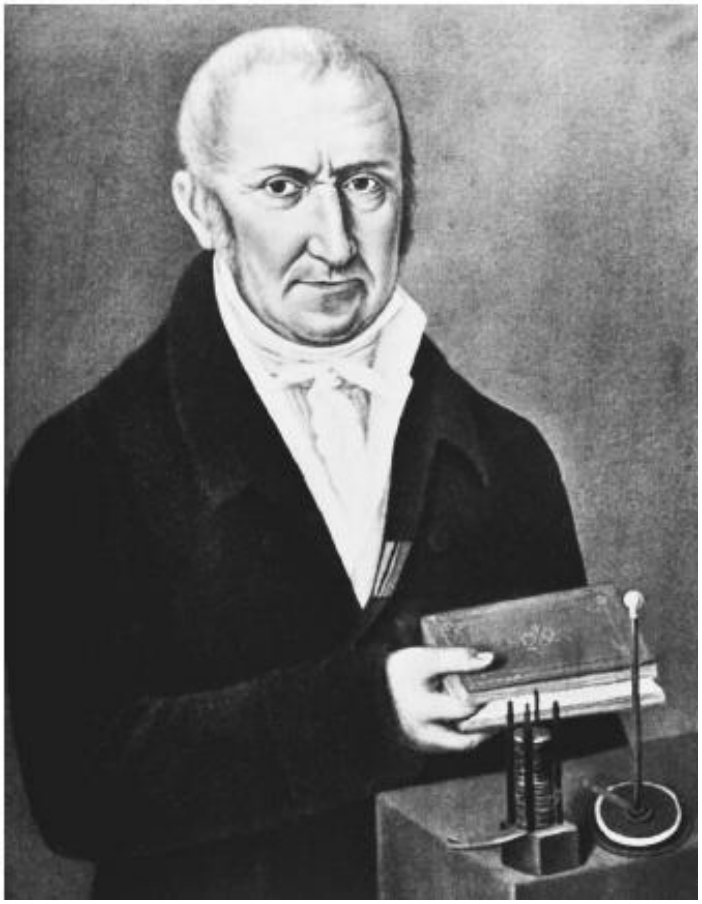

Alessandro Volta (1745-1827)

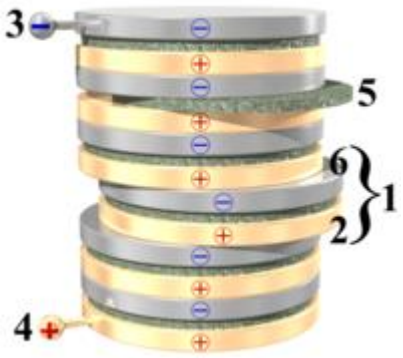

“vis electrica” esterna

Rane, torpedini e scintille. Galvani, Volta e l'elettricità animale
Marco Piccolino, Marco Bresadola
Bollati Boringhieri

I fluidi della vita. Alle origini della controversia sull'elettricità animale.
Walter Bernardi
Olschki Editore

La rana ambigua
Marcello Pera
Einaudi

Creative Education
2012. Vol.3, Special Issue, 1130-1137
Published Online October 2012 in SciRes (http://www.SciRP.org/journal/ce)
Scientific Research
DOI:10.4236/ce.2012.326169

A Computational View of the Historical Controversy on Animal Electricity

Massimiliano Zaniboni
Department of Biosciences, and Center of Excellence for Toxicological Research (CERT),
University of Parma, Parma, Italy
Email: massimiliano.zaniboni@unipr.it

Alan Hodgkin
(1914-1998)

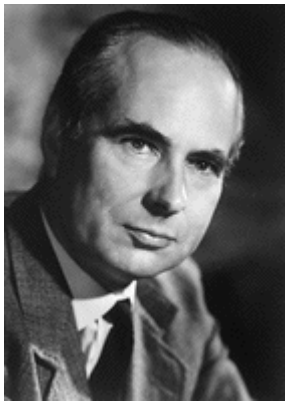

Andrew Huxley
(1917-2012)

1932-1936. Studia a Cambridge **storia naturale**, **matematica** e **fisica** al Trinity College, frequentato allora, fra gli altri, da Thompson, Rutherford, Hardy, Adrian, che esercitano tutti una profonda influenza su di lui.
Studia la teoria del cavo e i primi amplificatori.
1937-1938. Al Rockfeller Institute di New York impara con Cole e Hole a dissezionare l'assone gigante del calamaro.

1935. Studia **fisica**, **chimica** e **matematica** a Cambridge.
1938-39. Studia fisiologia sempre a Cambridge.
1939. Primi esperimenti con Hodgkin su registrazioni intracellulari da assone gigante di calamaro.
1940. Interrompe gli studi in medicina a causa dei primi bombardamenti

1940-1945. Collaborano a **un progetto sullo sviluppo di radar aerotrasportati**

Dopo la guerra tornano a Cambridge dove insegnano Fisiologia

1946-1951. Collaborano in esperimenti su fibre nervose giganti presso la Marine Station di Plymouth

La **MEMBRANA CELLULARE** è **ELETTRICAMENTE POLARIZZATA**

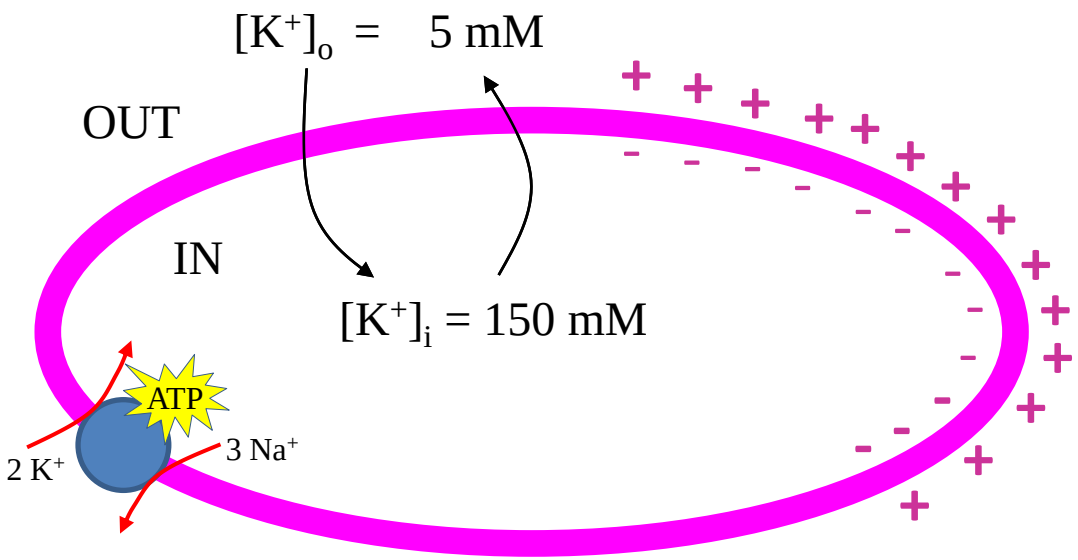

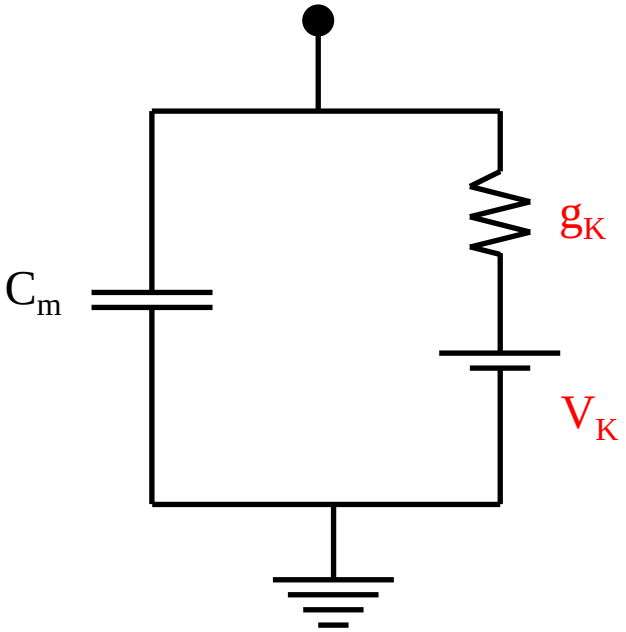

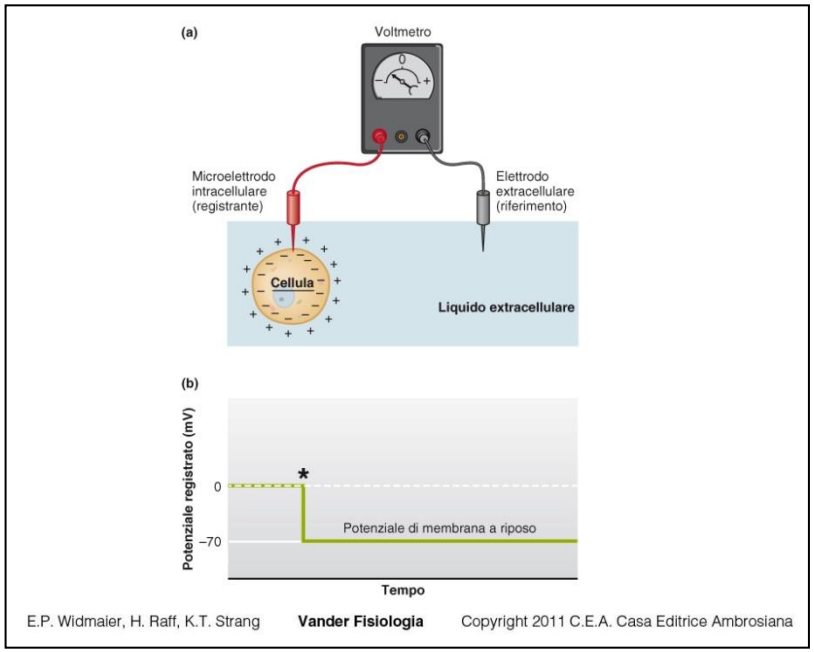

$$V_K = \frac{RT}{(+1)F} \ln \frac{[K^+]_o}{[K^+]_i} \sim -98 \text{ mV}$$

$$C\frac{dV}{dt} = i_m - g_K\left(V - V_K\right)$$

CELLULE ECCITABILI

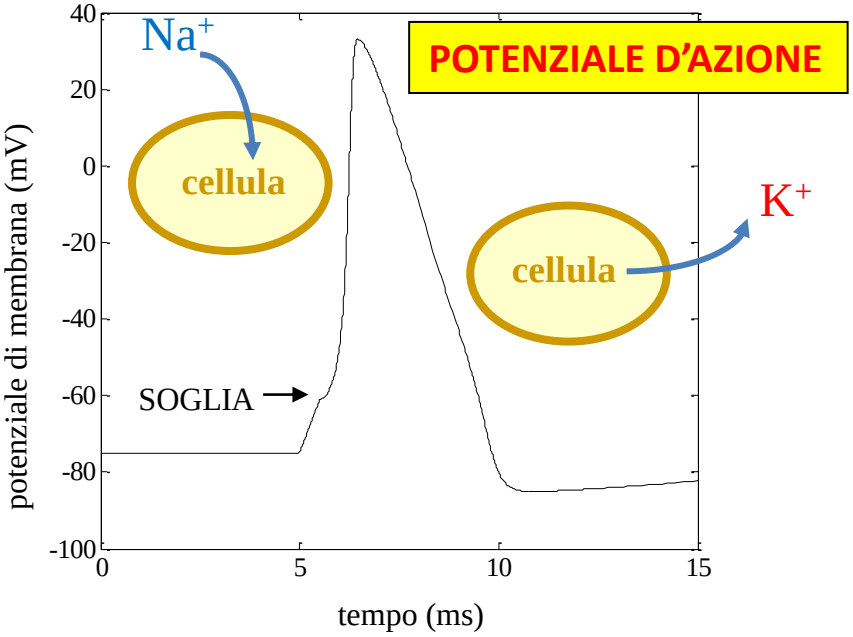

POTENZIALE D'AZIONE LOCALE

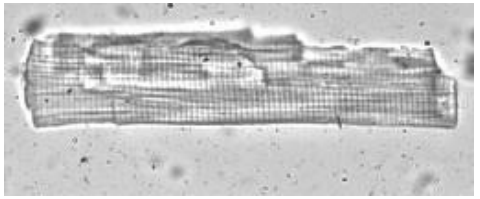

POTENZIALE D'AZIONE PROPAGATO

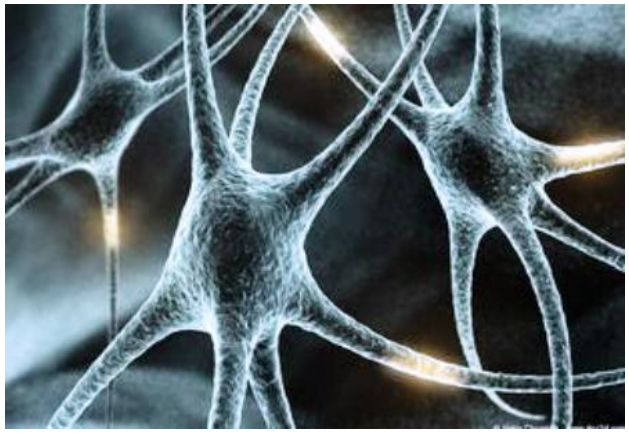

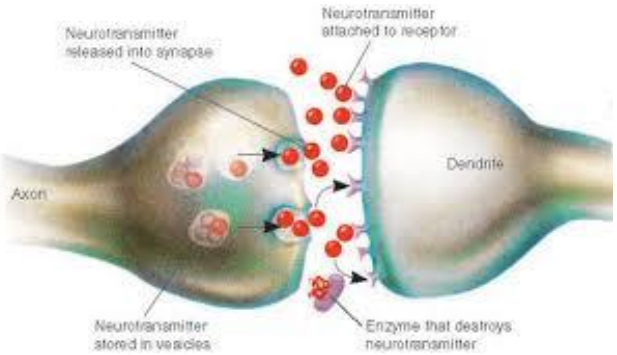

Sinapsi chimiche

CORRENTI ELETTROTONICHE

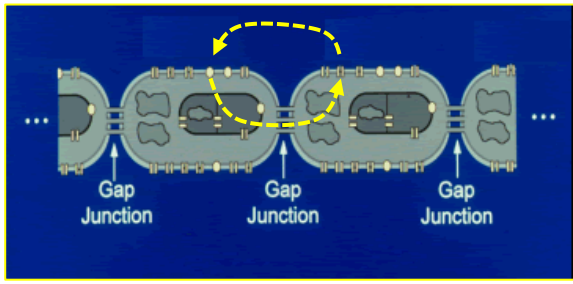

Sinapsi elettriche

CELLULE ECCITABILI

Sistema cardiocircolatorio

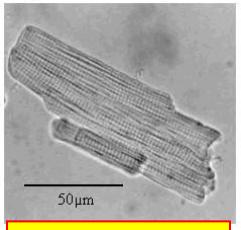

muscolo cardiaco

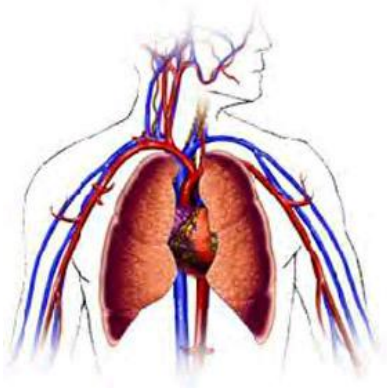

Sistema muscolo-scheletrico

muscolo scheletrico

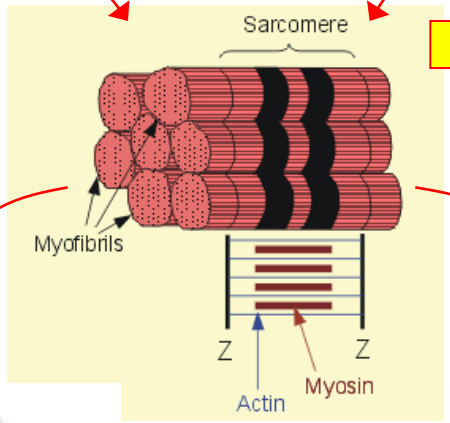

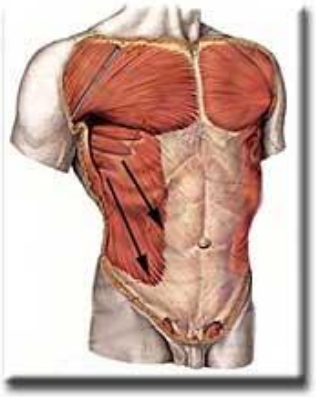

Vasi, organi interni, sfinteri …

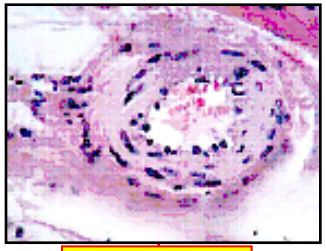

muscolo liscio

Sistema nervoso

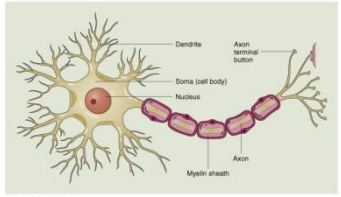

neuroni

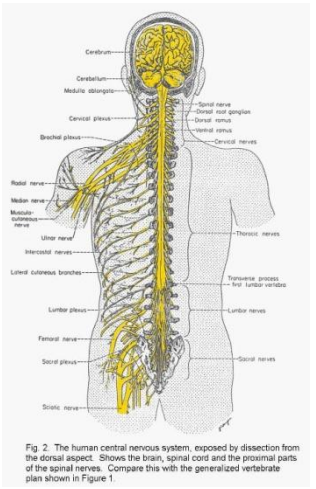

Fig. 2. The human central nervous system, exposed by dissection from the dorsal aspect. Shows the brain, spinal cord and the proximal parts of the spinal nerves. Compare this with the generalized vertebrate plan shown in Figure 1.

AMPLIFICATORE DIFFERENZIALE

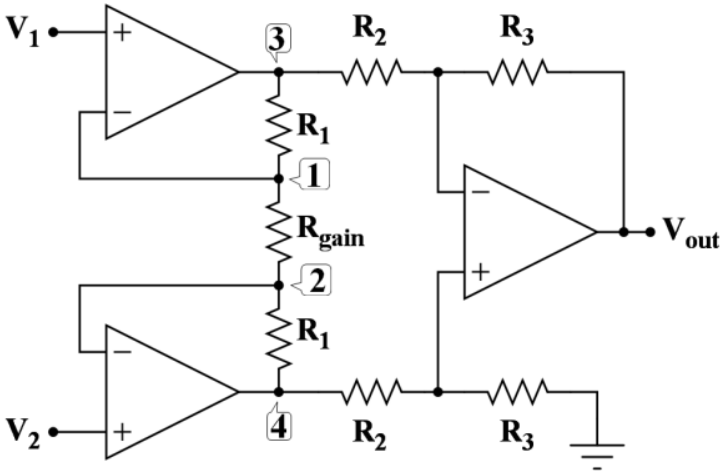


NERVE-CELL ENIGMA SOLVED

TECNICA DEL "**VOLTAGE-CLAMP**"

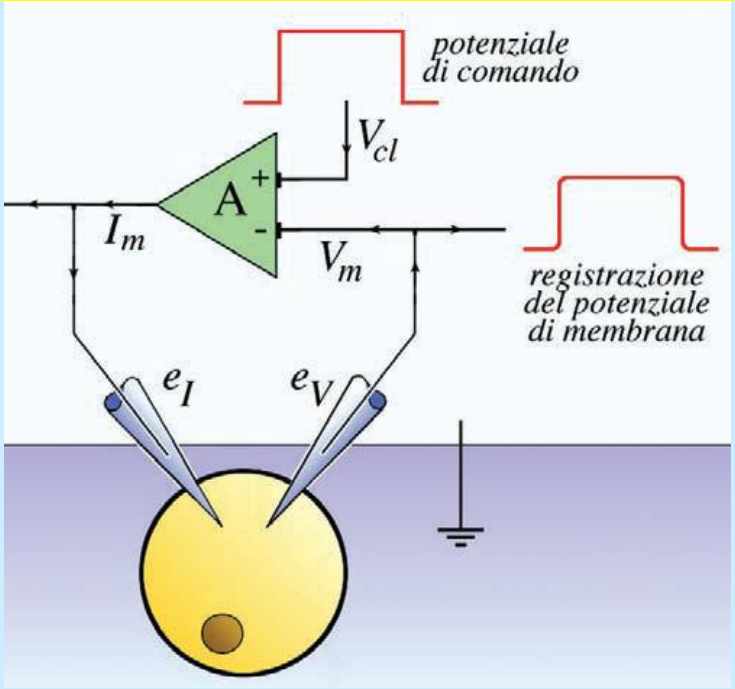

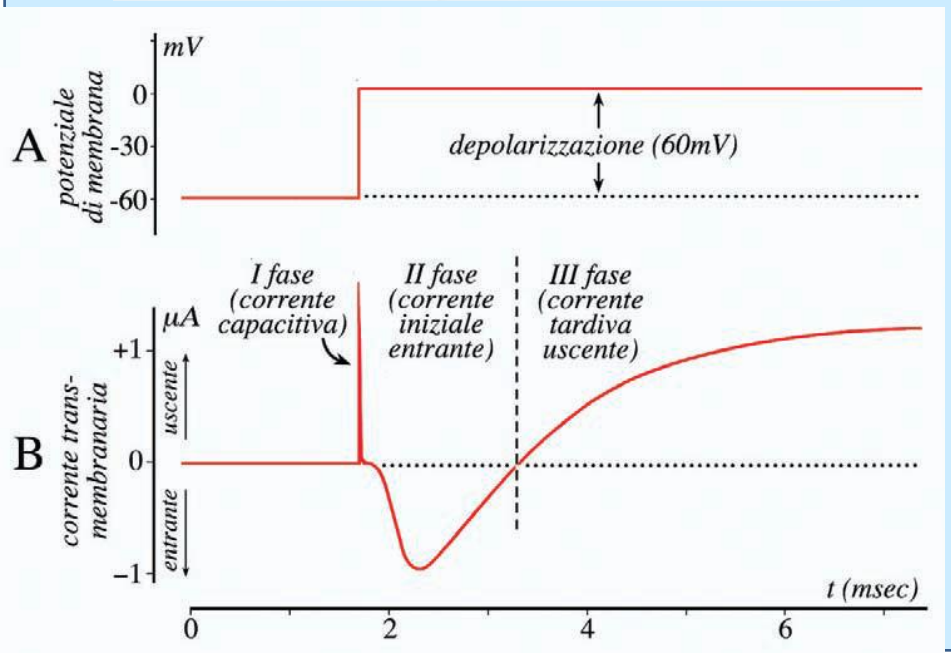

TECNICA DEL "**CURRENT-CLAMP**"

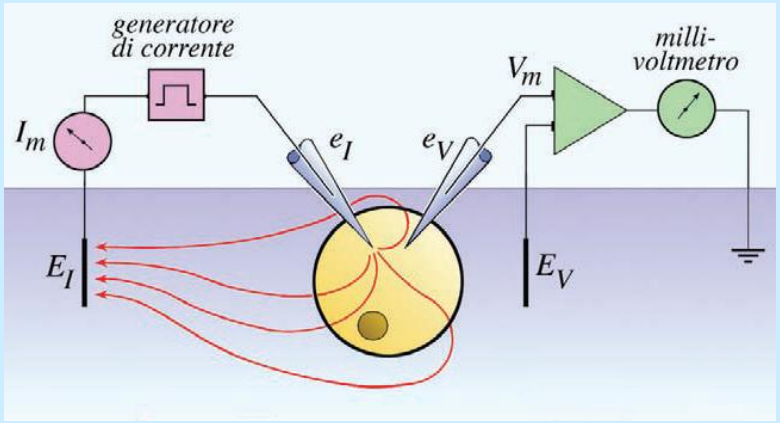

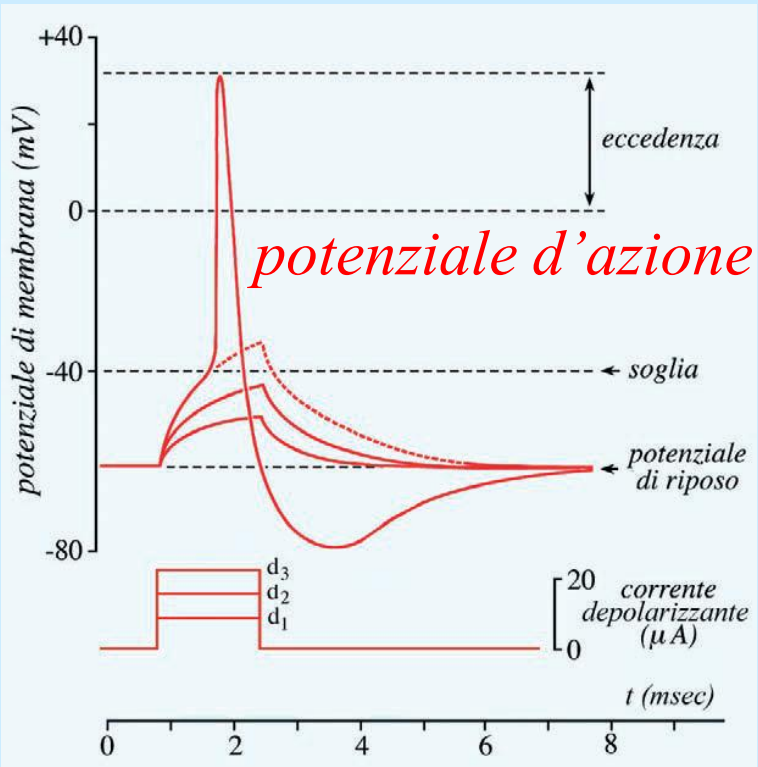

da **Taglietti e Casella**, Principi di Fisiologia e Biofisica delle Cellula

l'**ASSONE GIGANTE DEL CALAMARO (squid giant axon)**

(NERVO MEDIALE POSTERIORE)

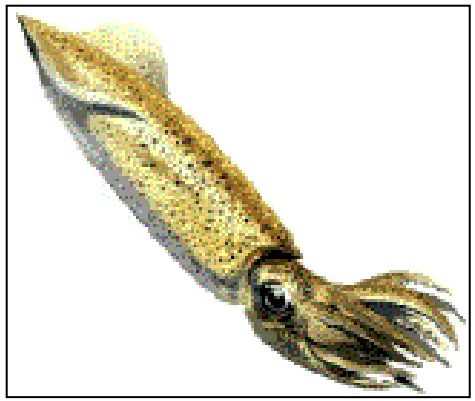

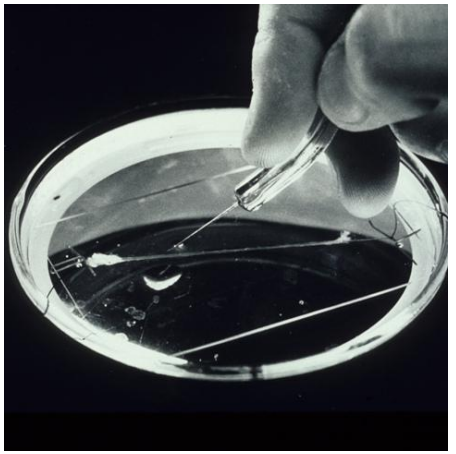

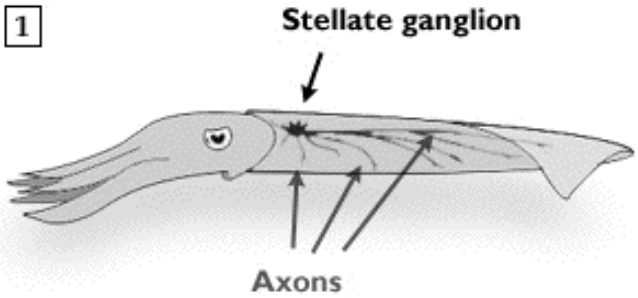

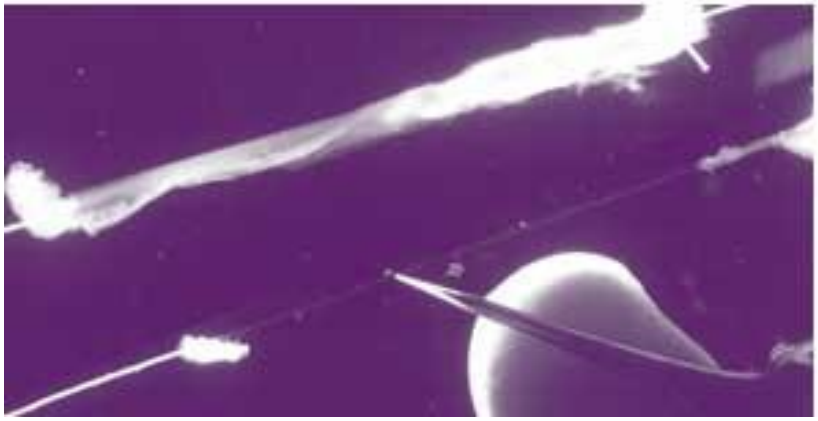

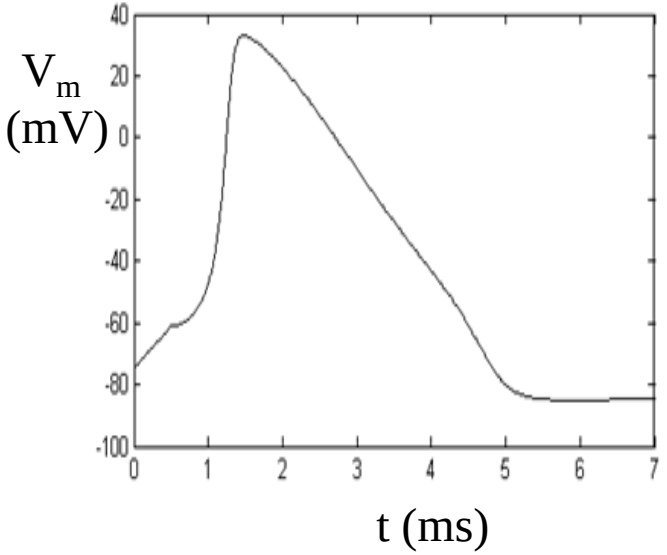

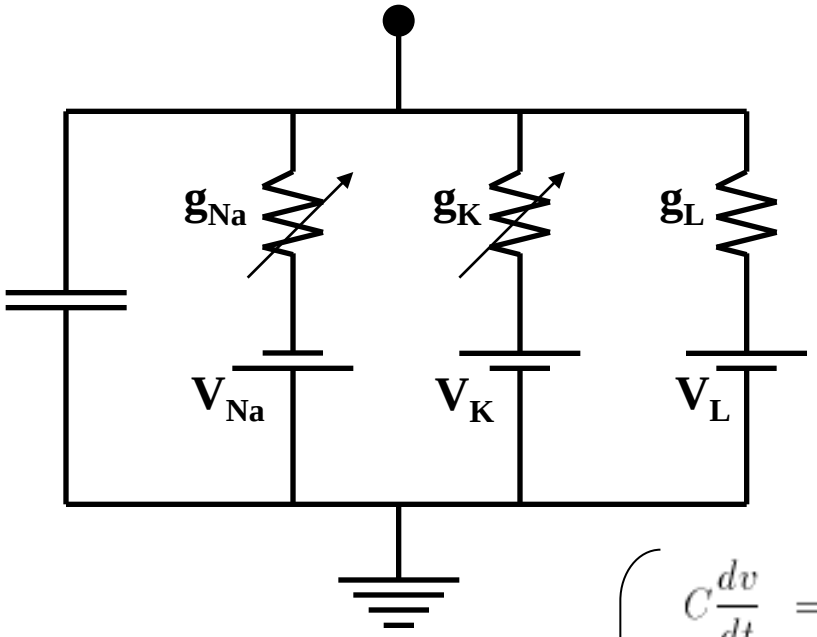

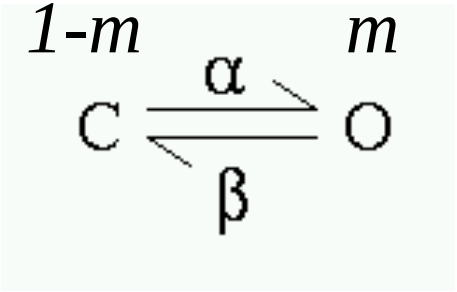

SISTEMA DI HODGKIN-HUXLEY

$$
\begin{aligned}
C\frac{dv}{dt} &= I - g_{Na}m^3h(V - V_{Na}) - g_K n^4(V - V_K) - g_L(V - V_L) \\
\frac{dm}{dt} &= a_m(V)(1-m) - b_m(V)m \\
\frac{dh}{dt} &= a_h(V)(1-h) - b_h(V)h \\
\frac{dn}{dt} &= a_n(V)(1-n) - b_n(V)n \\
a_m(V) &= .1(V+40)/(1-\exp(-(V+40)/10)) \\
b_m(V) &= 4\exp(-(V+65)/18) \\
a_h(V) &= .07\exp(-(V+65)/20) \\
b_h(V) &= 1/(1+\exp(-(V+35)/10)) \\
a_n(V) &= .01(V+55)/(1-\exp(-(V+55)/10)) \\
b_n(V) &= .125\exp(-(V+65)/80)
\end{aligned}
$$

Corrente di stimolo

CONTROVERSIA GALVANI-VOLTA

1950

days

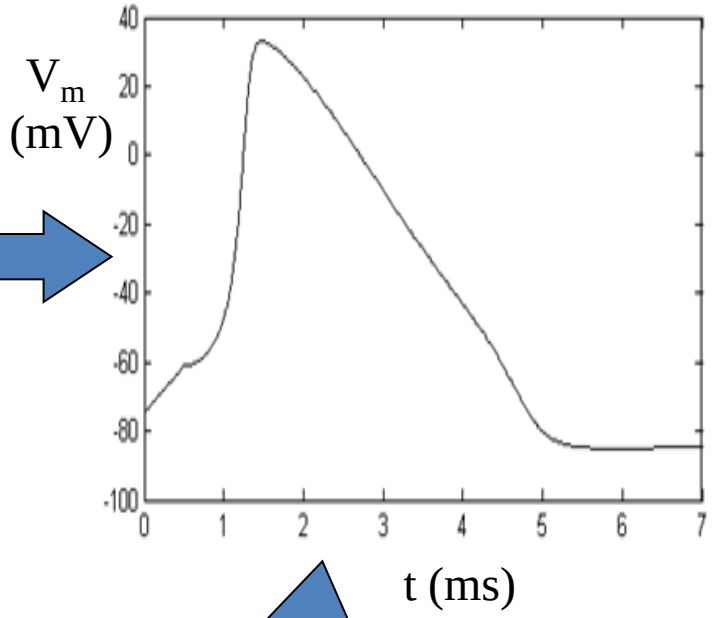

2014

$$
\begin{aligned}
C\frac{dv}{dt} &= I - g_{Na}m^3h(V - V_{Na}) - g_K n^4(V - V_K) - g_L(V - V_L) \\
\frac{dm}{dt} &= a_m(V)(1-m) - b_m(V)m \\
\frac{dh}{dt} &= a_h(V)(1-h) - b_h(V)h \\
\frac{dn}{dt} &= a_n(V)(1-n) - b_n(V)n \\
a_m(V) &= .1(V+40)/(1-\exp(-(V+40)/10)) \\
b_m(V) &= 4\exp(-(V+65)/18) \\
a_h(V) &= .07\exp(-(V+65)/20) \\
b_h(V) &= 1/(1+\exp(-(V+35)/10)) \\
a_n(V) &= .01(V+55)/(1-\exp(-(V+55)/10)) \\
b_n(V) &= .125\exp(-(V+65)/80)
\end{aligned}
$$

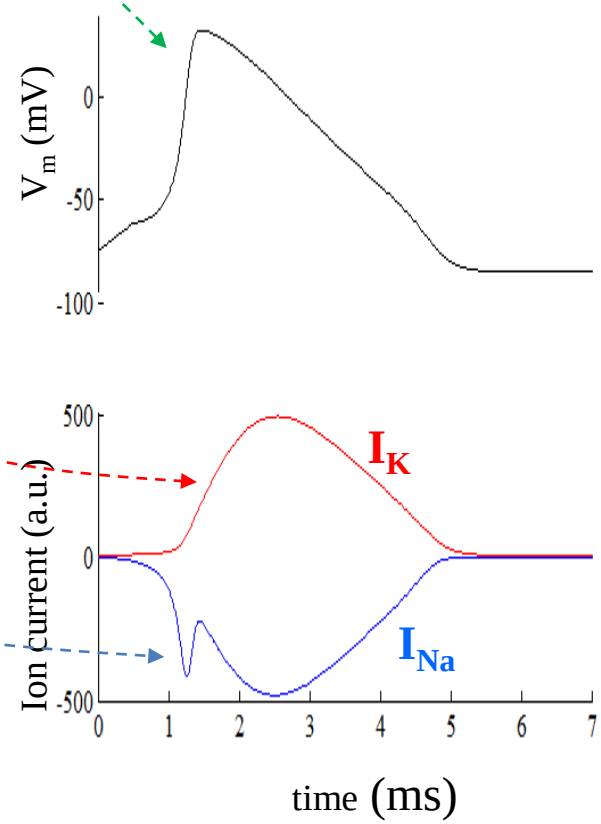

1952 – pubblicano il loro studio su due articoli storici su **Journal of Physiology**

1963 - Premio Nobel per la Fisiologia e Medicina con John Eccles.

PATCH CLAMP

Erwin Neher

Bert Sakmann

1991 - Premio Nobel per la Fisiologia e Medicina.

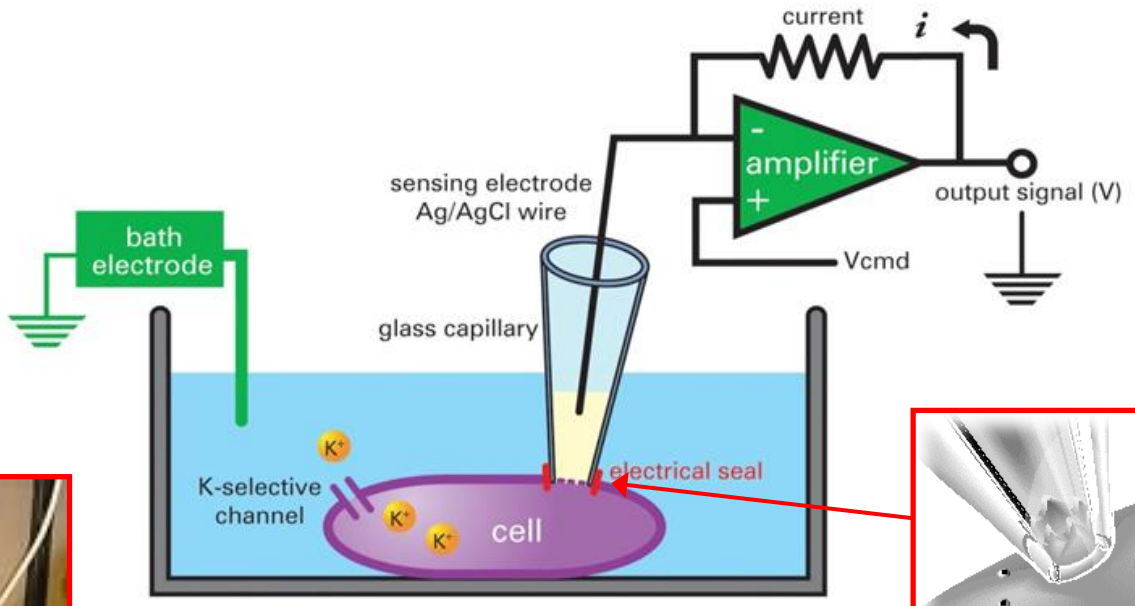

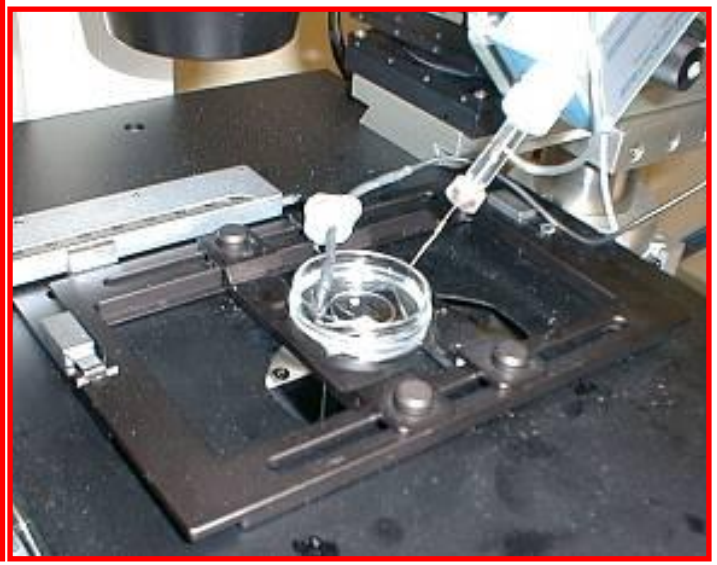

CANALI IONICI VOLTAGGIO-DIPENDENTI

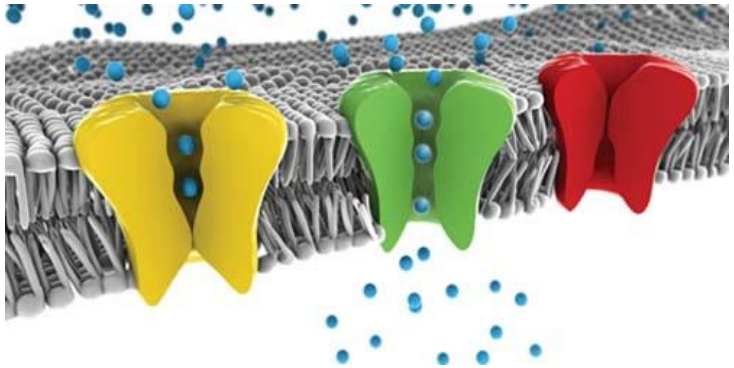

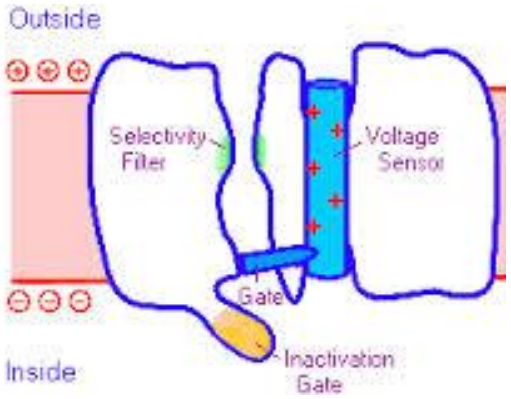

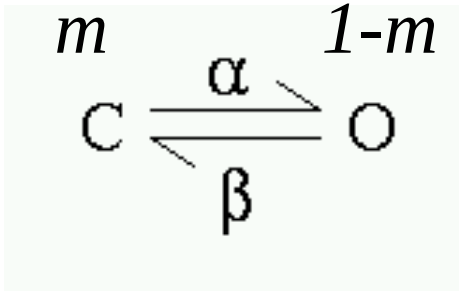

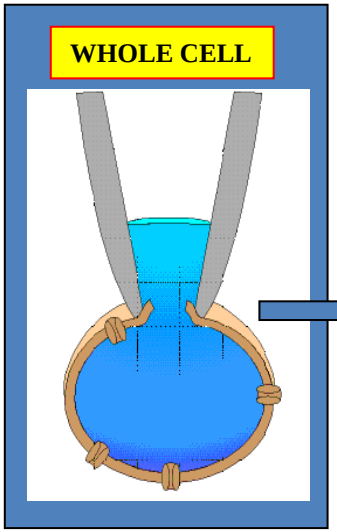

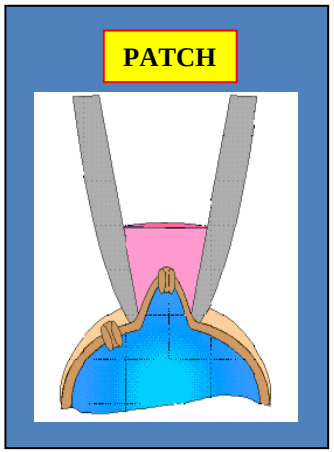

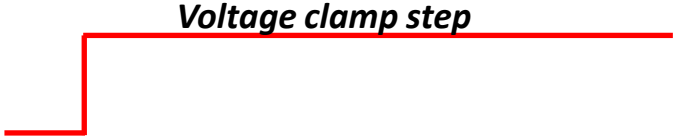

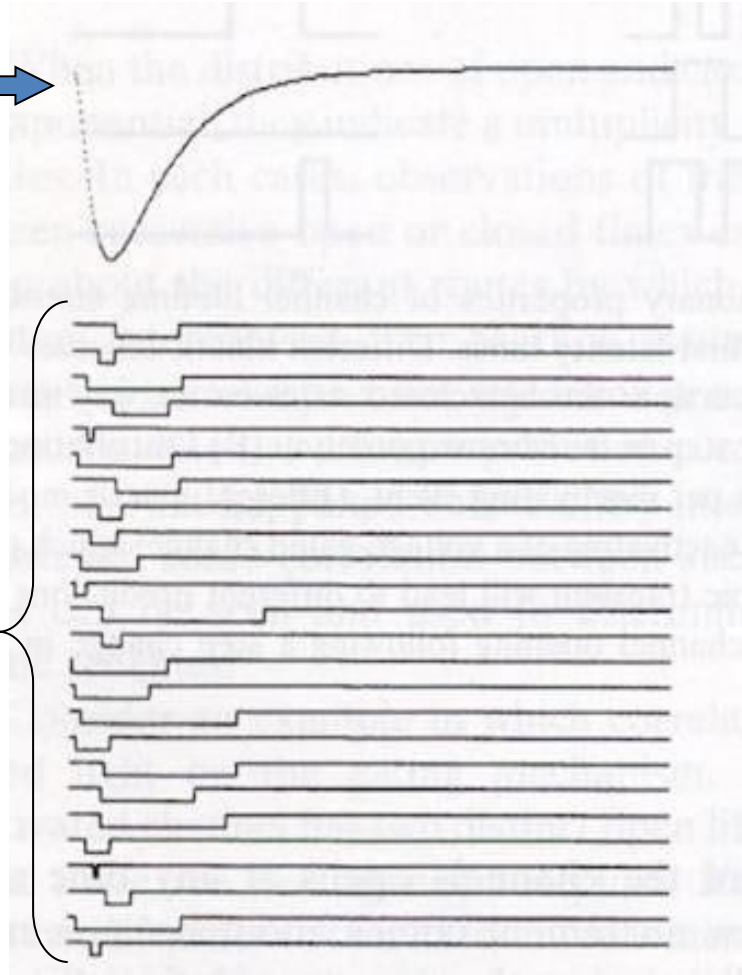

ACTION POTENTIAL CLAMP

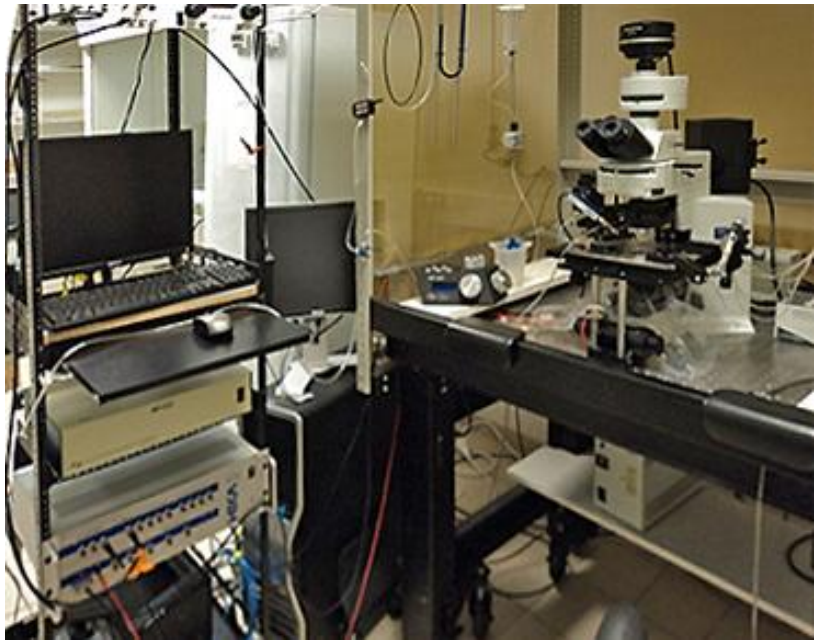

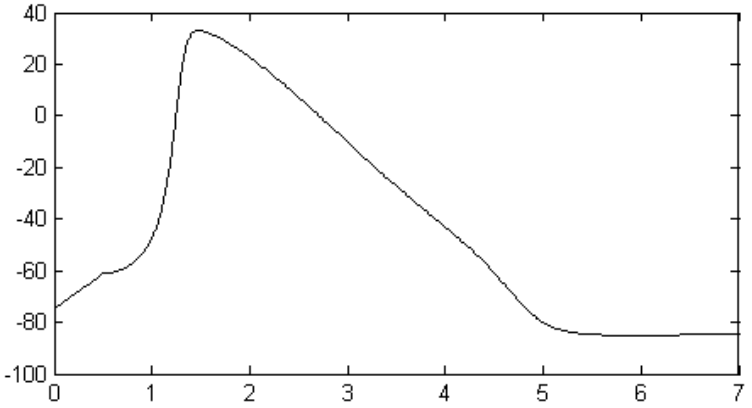

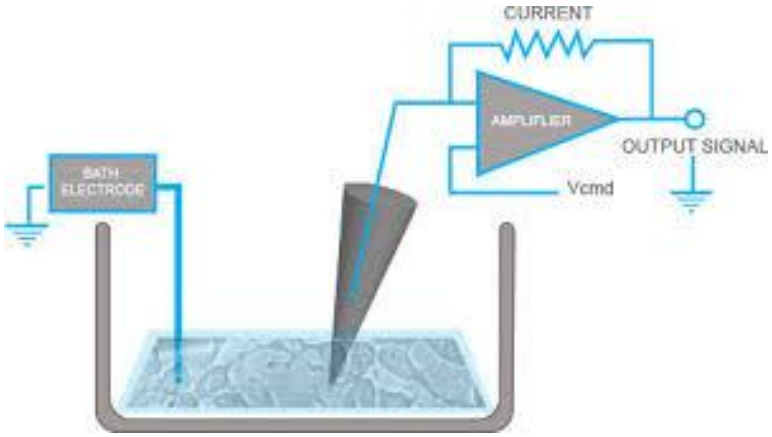

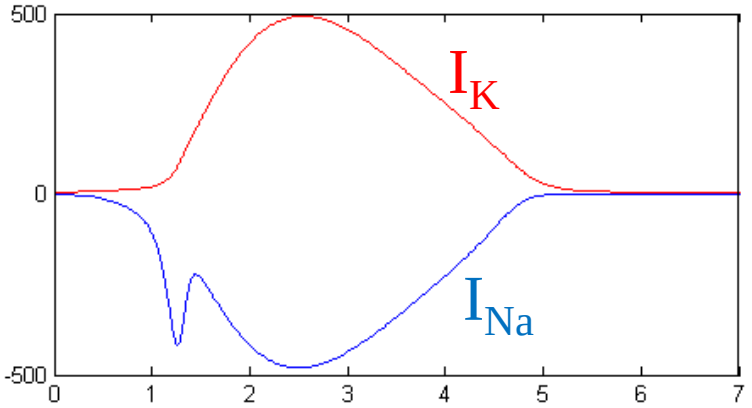

Tecniche di isolamento enzimatico cellulare

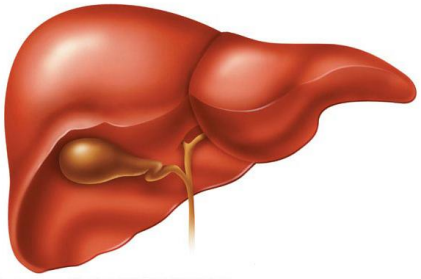

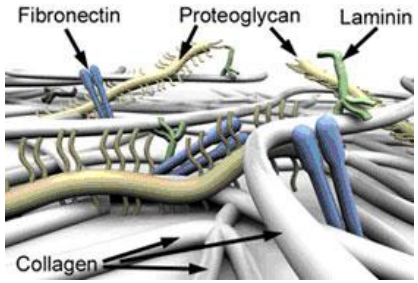

ENZIMI PROTEOLITICI

- Collagenase
- Protease
- Elastase
- …

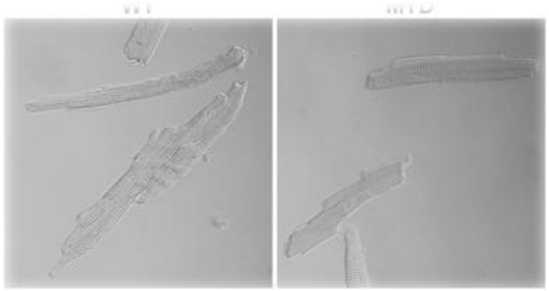

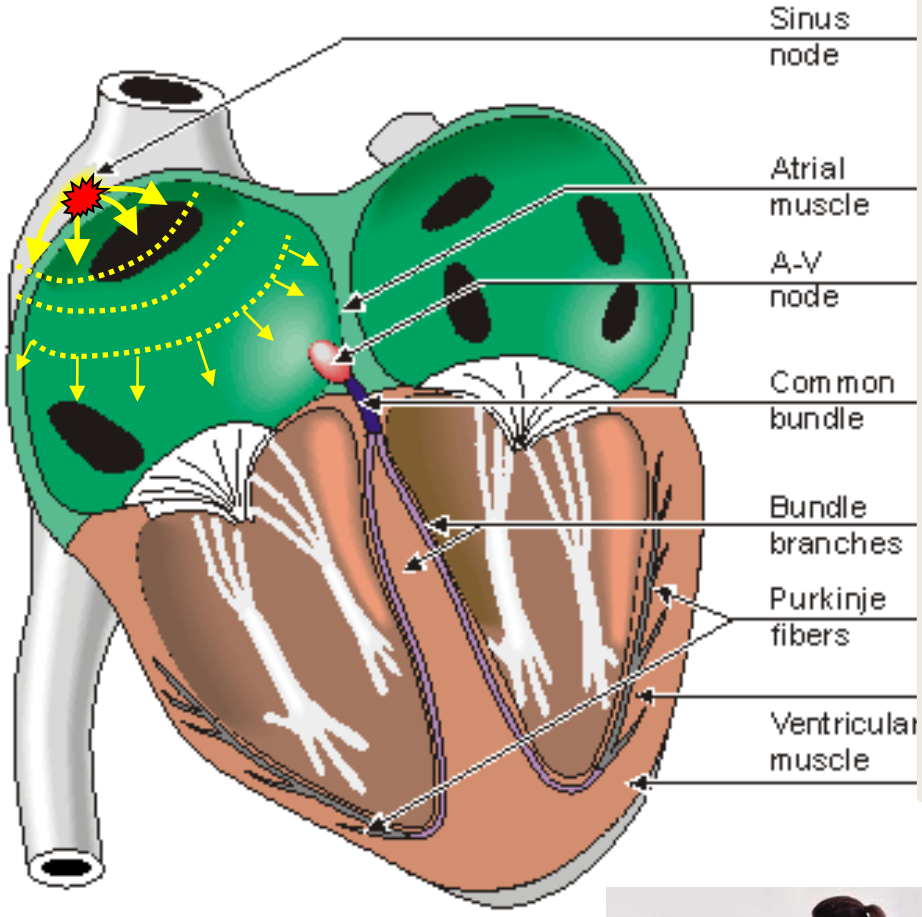
Sinus node
Atrial muscle
A-V node
Common bundle
Bundle branches
Purkinje fibers
Ventricular muscle

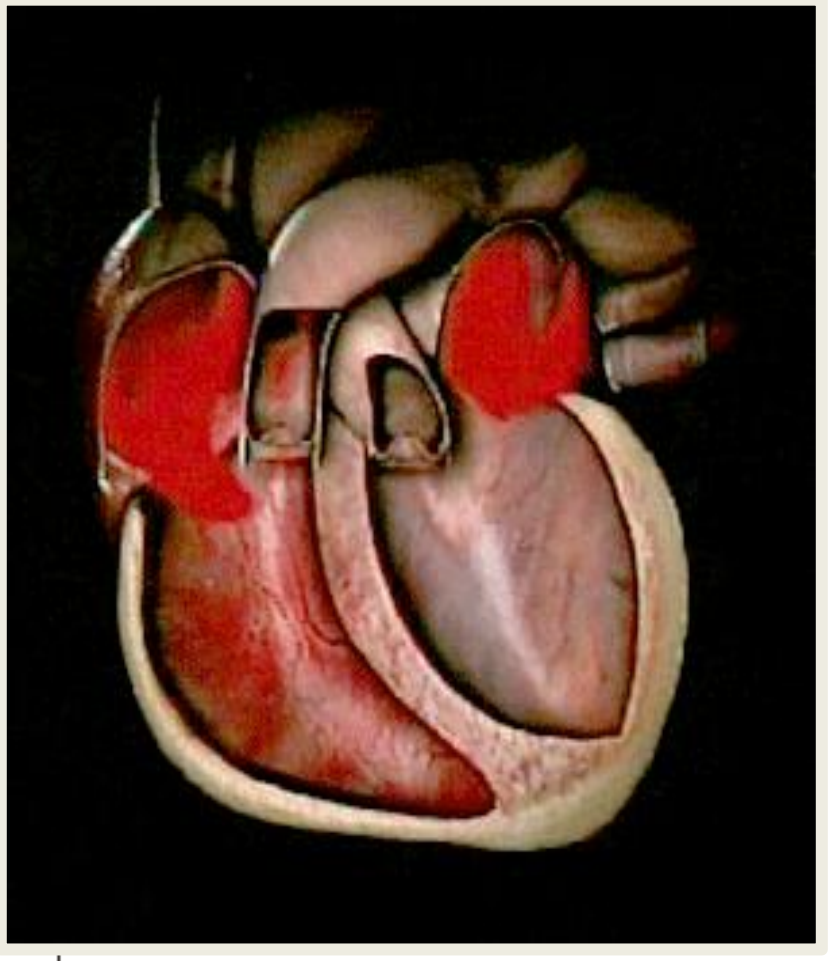

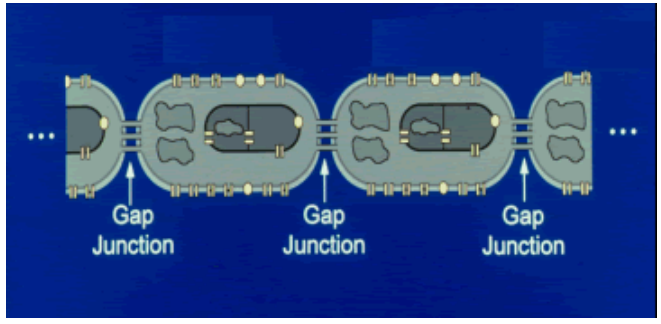
Gap Junction
Gap Junction
Gap Junction

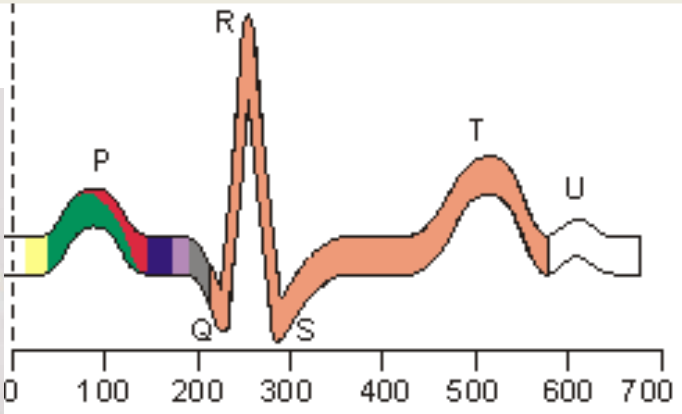
R
P
T
U
Q
S
0
100
200
300
400
500
600
700

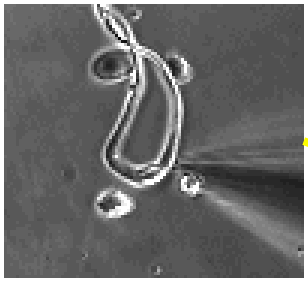

cellule pacemaker
nodo seno-atriale

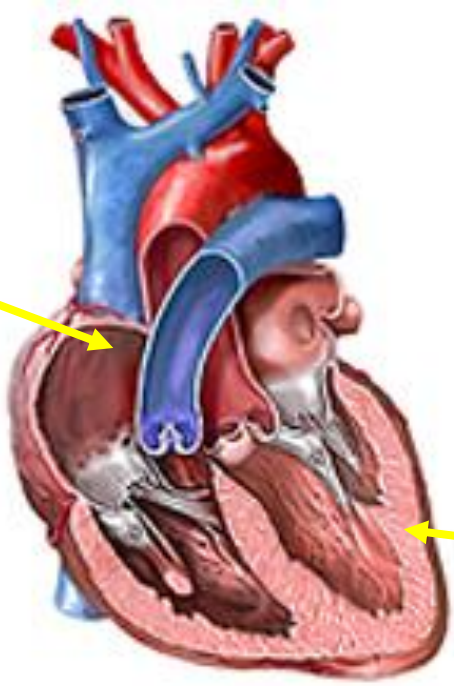

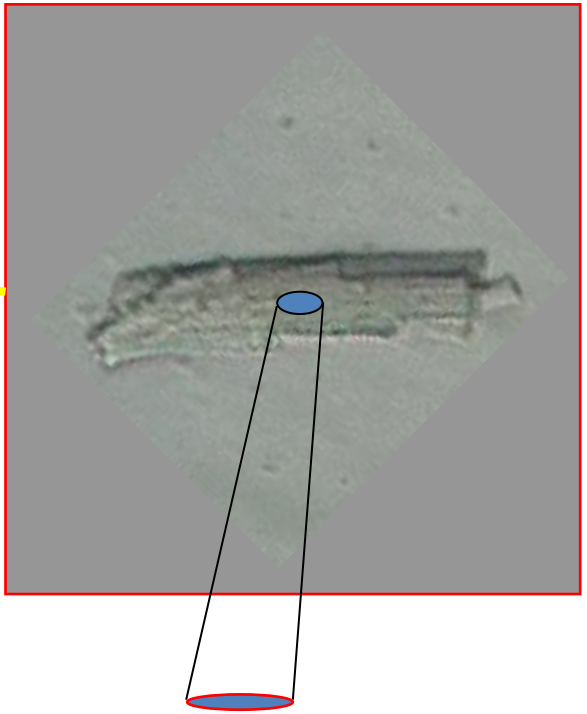

cellule muscolari
ventricolo

MODELLIZZAZIONE MATEMATICA DELL'ATTIVITA' ELETTRICA CARDIACA

Potenziale d'azione **ventricolare umano**

1. Priebe-Beuckelmann (1998)
2. Bernus et al. (2002)
3. Ten Tusscher et al. (2004)
4. Iyer-Mazhari-Winslow (2004)
5. Bueno et al. (2006)
6. …

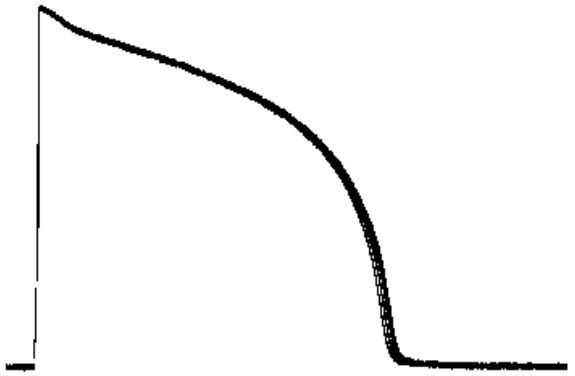

Potenziale d'azione **nodo seno-atriale di coniglio**

1. Yanagihara-Noma-Irisawa (1980)
2. Bristow-Clark (1982)
3. Irisawa-Noma (1982)
4. Noble-Noble (1984)
5. Noble-DiFrancesco-Denyer (1989)
6. Wilders-Jongsma-Van Ginneken (1991)
7. Demir-Clark-Murphey-Giles (1994)
8. Dokos-Celler-Lovell (1996)
9. Zhang et al (2000)
10. Kurata et al (2002)
11. Sarai et al (2003)
12. …

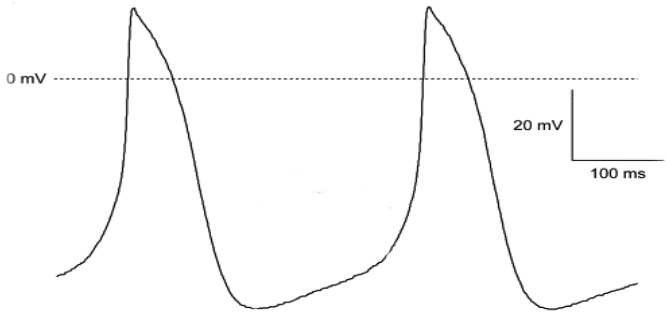

HUMAN VENTRICULAR ACTION POTENTIAL

Leo Priebe and Dirk J. Beuckelmann
Circ. Res. 1998;82;1206-1223

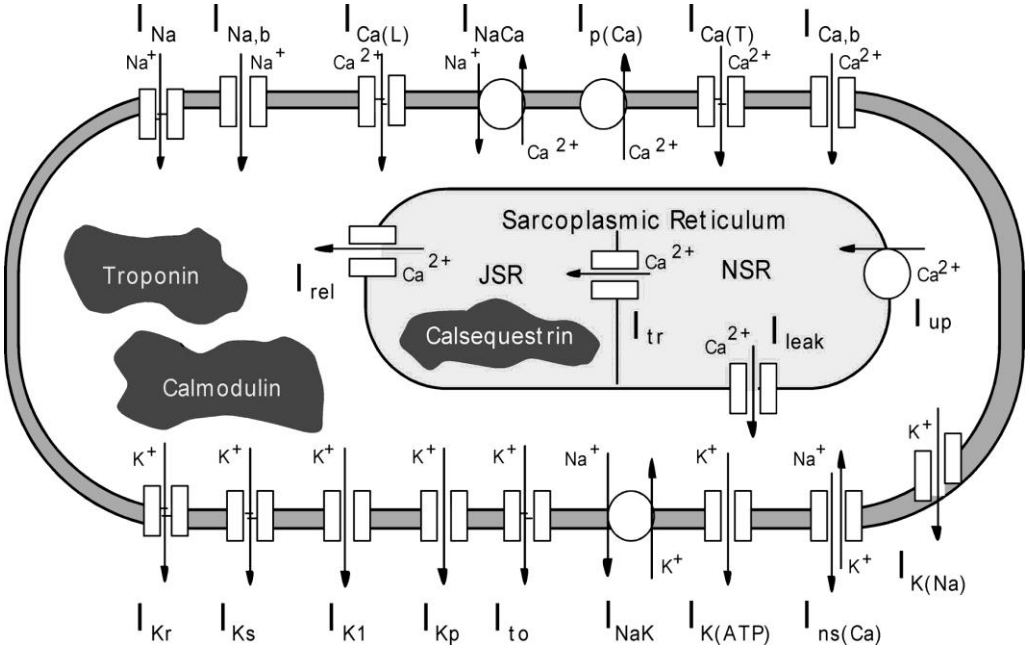

***Fast Na^+ Current:* I_{Na}**

$I_{Na}=16\cdot m^3\cdot h\cdot j\cdot(V-E_{Na})$

$E_{Na}=(RT/F)\cdot\ln([Na^+]_o/[Na^+]_i)$

where m, h, and j are the activation gate, the fast inactivation gate, and the slow inactivation gate of I_{Na}, respectively, V is the membrane potential, E_{Na} is the equilibrium potential for Na^+, R is the universal gas constant, T is the absolute temperature, and F is the Faraday constant.

For $V\geq -40$ mV

$\alpha_h=\alpha_j=0.0$

$\beta_h=1/\left(0.13\cdot\{1+\exp[(V+10.66)/-11.1]\}\right)$

$\beta_j=0.3\cdot\exp(-2.535\cdot10^{-7}\cdot V)/\{1+\exp[-0.1\cdot(V+32)]\}$

For $V<-40$ mV

$\alpha_h=0.135\cdot\exp[(80+V)/-6.8]$

$\beta_h=3.56\cdot\exp(0.079\cdot V)+3.1\cdot10^5\cdot\exp(0.35\cdot V)$

$\alpha_j=[-1.2714\cdot10^5\cdot\exp(0.244\cdot V)-3.474\cdot10^{-5}$

$\cdot\exp(-0.04391\cdot V)]\cdot(V+37.78)/\{1+\exp[0.311\cdot(V+79.23)]\}$

$\beta_j=0.1212\cdot\exp(-0.01052\cdot V)/\{1+\exp[-0.1378\cdot(V+40.14)]\}$

For the total range of V

$\alpha_m=0.32\cdot(V+47.13)/\{1-\exp[-0.1\cdot(V+47.13)]\}$

$\beta_m=0.08\cdot\exp(-V/11)$

***Slow Inward Current:* I_{Ca}**

$I_{Ca}=g_{Ca,max}\cdot d\cdot f\cdot f_{Ca}\cdot(V-E_{Ca})$

$g_{Ca,max}=0.064$ mS/μF

$E_{Ca}=(RT/2F)\cdot\ln([Ca^{2+}]_o/[Ca^{2+}]_i)$

$\alpha_d=14.98/(16.68\cdot\sqrt{2\cdot\pi})\exp\{-[(V-22.36)/16.68]^2/2\}$

$\beta_d=0.1471-5.3/(14.93\cdot\sqrt{2\cdot\pi})\exp\{-[(V-6.27)/14.93]^2/2\}$

$\alpha_f=[6.87\cdot10^{-3}]/\{1+\exp[(6.1546-V)/-6.12]\}$

$\beta_f=\{0.069\cdot\exp[-0.11\cdot(V+9.825)]+0.011\}/$

$\{1+\exp[-0.278\cdot(V+9.825)]\}-5.75\cdot10^{-4}$

$f_{Ca}=1/(1+([Ca^{2+}]_i/K_{Ca}))$

$K_{Ca}=600$ nmol/L

where $g_{Ca,max}$ is g_{max} for I_{Ca}, d is the activation gate of I_{Ca}, f is the inactivation gate of I_{Ca}, E_{Ca} is the equilibrium potential for Ca^{2+}, f_{Ca} is a proportional factor for Ca^{2+}-dependent inactivation of I_{Ca}, and K_{Ca} is half-maximum Ca^{2+} binding concentration for I_{Ca}.

Outward Current

Transient Outward Current: I_{to}

$I_{to}=g_{to,max}\cdot r\cdot t\cdot(V-E_{to})$

$E_{to}=(RT/F)\cdot\ln\{(0.043\cdot[Na^+]_o+[K^+]_o)/(0.043\cdot[Na^+]_i+[K^+]_i)\}$

$g_{to,max}$: nonfailing⇒0.3 mS/μF; heart failure⇒0.191 mS/μF

$\alpha_r=\{0.5266\cdot\exp[-0.0166\cdot(V-42.2912)]\}/$

$\{1+\exp[-0.0943\cdot(V-42.2912)]\}$

$\beta_r=\{0.5149\cdot\exp[-0.1344\cdot(V-5.0027)]+5.186\cdot10^{-5}\cdot V\}/$

$\{1+\exp[-0.1348\cdot(V-5.186\cdot10^{-5})]\}$

$\alpha_t=\{0.0721\cdot\exp[-0.173\cdot(V+34.2531)]+5.612\cdot10^{-5}\cdot V\}/$

$\{1+\exp[-0.1732\cdot(V+34.2531)]\}$

$\beta_t=\{0.0767\cdot\exp[-1.66\cdot10^{-9}\cdot(V+34.0235)]+1.215\cdot10^{-4}\cdot V\}/$

$\{1+\exp[-0.1604\cdot(V+34.0235)]\}$

where $g_{to,max}$ is g_{max} for I_{to}, r and t are the activation gate and the inactivation gate of I_{to}, respectively, and E_{to} is the equilibrium potential for I_{to}.

Delayed Rectifier Current

Slowly Activating Current: I_{Ks}

$I_{Ks}=g_{Ks,max}\cdot X_s^2\cdot(V-E_K)$

$E_{Ks}=(RT/F)\cdot\ln\{(0.01833\cdot[Na^+]_o+[K^+]_o)/(0.01833\cdot[Na^+]_i+[K^+]_i)\}$

$g_{Ks,max}=0.02$ mS/μF

$\alpha_{X_s}=3.0\cdot10^{-3}/\{1+\exp[(7.44-(V+10)/14.32]\}$

$\beta_{X_s}=5.87\cdot10^{-3}/\{1+\exp[(-5.95-(V+10)/-15.82]\}$

where $g_{Ks,max}$ is g_{max} for I_{Ks}, X_s is the activation gate of I_{Ks}, and E_{Ks} is the equilibrium potential for I_{Ks}.

Rapidly Activating Current: I_{Kr}

$I_{Kr}=g_{Kr,max}\cdot Xr\cdot rik\cdot(V-E_K)$

$E_K=(RT/F)\cdot\ln([K^+]_o/[K^+]_i)$

$g_{Kr,max}=0.015$ mS/μF

$\alpha_{Xr}=\{0.005\cdot\exp[5.266\cdot10^{-4}\cdot(V+4.067)]\}/$

$\{1+\exp[-0.1262\cdot(V+4.067)]\}$

$\beta_{Xr}=\{0.016\cdot\exp[1.6\cdot10^{-3}\cdot(V+65.66)]\}/$

$\{1+\exp[0.0783\cdot(V+65.66)]\}$

$rik=1/\{1+\exp[(V+26)/23]\}$

where $g_{Kr,max}$ is g_{max} for I_{Kr}, Xr is the activation gate of I_{Kr}, rik is the inward-rectification factor of I_{Kr}, and E_K is the equilibrium potential for I_K.

Inward Rectifier Current: I_{K1}

$I_{K1}=g_{K1,max}\cdot K1_\infty\cdot(V-E_{K1})$

$E_{K1}=(RT/F)\cdot\ln([K^+]_o/[K^+]_i)$

$g_{K1,max}$: nonfailing⇒2.5 mS/μF; heart failure⇒2.0 mS/μF

$\alpha_{K1}=0.1/\{1+\exp[0.06\cdot(V-E_{K1}-200)]\}$

$\beta_{K1}=\{3\cdot\exp[2\cdot10^{-4}\cdot(V-E_{K1}+100)]+\exp[0.1\cdot(V-E_{K1}-10)]\}/$

$\{1+\exp[-0.5\cdot(V-E_{K1})]\}$

$K1_\infty=\alpha_{K1}/(\alpha_{K1}+\beta_{K1})$

where $g_{K1,max}$ is g_{max} for I_{K1}, $K1_\infty$ is the inactivation gate of I_{K1}, and E_{K1} is the equilibrium potential for I_{K1}.

Background Currents

Ca^{2+} Background Current: $I_{Ca,b}$

$I_{Ca,b}=\overline{G}_{Ca,b}\cdot(V-E_{Ca,b})$

$\overline{G}_{Ca,b}$: nonfailing⇒0.00085 mS/μF; heart failure⇒0.0013 mS/μF

$E_{Ca,b}=E_{Ca}$

where $\overline{G}_{Ca,b}$ is g_{max} for $I_{Ca,b}$, and $E_{Ca,b}$ is the equilibrium potential for $I_{Ca,b}$.

Na^{+} Background Current: $I_{Na,b}$

$I_{Na,b}=\overline{G}_{Na,b}\cdot(V-E_{Na,b})$

$\overline{G}_{Na,b}$: nonfailing⇒0.001 mS/μF; heart failure⇒0 mS/μF

$E_{Na,b}=E_{Na}$

where $\overline{G}_{Na,b}$ is g_{max} for $I_{Na,b}$, and $E_{Na,b}$ is the equilibrium potential for $I_{Na,b}$.

Pump and Exchanger

Na^{+}-K^{+} Pump: I_{NaK}

$I_{NaK}=\bar{I}_{NaK}\cdot f_{NaK}\cdot 1/(1+(K_{m,Na_i}/[Na^{+}]_i)^{1.5})\cdot[[K^{+}]_o/([K^{+}]_o+K_{m,K_o})]$

$\bar{I}_{NaK}$: nonfailing⇒1.3 pA/pF; heart failure⇒0.75 pA/pF

$f_{NaK}=1/[1+0.1245\cdot\exp(-0.1\cdot V\cdot F/RT)$

$+0.0365\cdot\sigma\cdot\exp(-V\cdot F/RT)]$

$\sigma=1/7\cdot\{\exp([Na^{+}]_o/67.3)-1\}$

$K_{m,Na_i}=10$ mmol/L

$K_{m,K_o}=1.5$ mmol/L

where f_{NaK} is the voltage-dependence parameter of I_{NaK}, and σ is the $[Na^{+}]_o$-dependence factor of I_{NaK}.

Na^{+}-Ca^{2+} Exchanger Current: I_{NaCa}

$I_{NaCa}=k_{NaCa}\cdot(K^3_{m,Na}+[Na^{+}]^3_o)^{-1}\cdot(K_{m,Ca}+[Ca^{2+}]_o)^{-1}$

$\cdot(1+k_{sat}\cdot\exp[(\eta-1)\cdot V\cdot F/(RT)])^{-1}\cdot\{\exp[\eta\cdot V\cdot F/(RT)]$

$\cdot[Na^{+}]^3_i\cdot[Ca^{2+}]_o-\exp[(\eta-1)\cdot V\cdot F/(RT)]\cdot[Na^{+}]^3_o\cdot[Ca^{2+}]_i\}$

k_{NaCa}: nonfailing⇒1000 pA/pF; heart failure⇒1650 pA/pF

$K_{m,Na}=82.5$ mmol/L; $K_{m,Ca}=1.38$ mmol/L; $k_{sat}=0.1$; $\eta=0.35$

where k_{sat} is the saturation factor of I_{NaCa} at very negative potentials, and η is the position of the energy barrier controlling voltage dependence of I_{NaCa}.

Ca^{2+} Homeostasis

CICR of JSR

$I_{rel}=G_{rel}([Ca^{+}]_{JSR}-[Ca^{2+}]_i)$ in mmol/L per ms

$G_{rel}=\overline{G}_{rel}\{\Delta[Ca^{2+}]_{i,2}-\Delta[Ca^{2+}]_{i,th}/(K_{m,rel}+\Delta[Ca^{2+}]_{i,2}-\Delta[Ca^{2+}]_{i,th})\}$

$\cdot(1-\exp[-t/\tau_{on}])\cdot\exp[-t/\tau_{off}]$

$\Delta[Ca^{2+}]_{i,2}=\Sigma$ calcium−influx during first 2 ms after initiation of AP

$\Delta[Ca^{2+}]_{i,th}=0.005$ μmol/L

$K_{m,rel}=0.8$ μmol/L

$\tau_{on}=\tau_{off}=4$ ms; t=0 at time of CICR

$\overline{G}_{rel}=22$ ms^{-1}

where I_{rel} is the SR Ca^{2+} release current, and G_{rel} is the rate constant of Ca^{2+} release from JSR.

Spontaneous Ca^{2+} Release of JSR

$I_{rel}=G_{rel}([Ca^{2+}]_{JSR}-[Ca^{2+}]_i)(1-\exp[-t/\tau_{on}])\cdot\exp[-t/\tau_{off}]$

in mmol/L per ms

$G_{rel}=3\ ms^{-1}$

$\tau_{on}=\tau_{off}=4$ ms; t=0 at time of CICR

Ca^{2+} Uptake and Leakage of NSR: I_{up} and I_{leak}

$I_{up}=\bar{I}_{up}[Ca^{2+}]_i/([Ca^{2+}]_i+K_{m,up})$ in mmol/L per ms

$I_{leak}=K_{leak}[Ca^{2+}]_{NSR}$ mmol/L per ms

$\bar{I}_{up}$: nonfailing⇒0.0045; heart failure⇒0.0015 in mmol/L per ms

$K_{m,up}=0.92\ \mu$mol/L

K_{leak}: nonfailing⇒0.00026 ms^{-1}; heart failure⇒0.00017 ms^{-1}

where I_{up} is the SR Ca^{2+} uptake current, and I_{leak} is the leakage current.

Translocation of Ca^{2+} From NSR to JSR: I_{tr}

$I_{tr}=([Ca^{2+}]_{NSR}-[Ca^{2+}]_{JSR})/\tau_{tr}$ in mmol/L per ms

$\tau_{tr}=180$ ms

where I_{tr} is the SR Ca^{2+} translocation current.

Ca^{2+} Buffers in the Myoplasm: Troponin (TRPN) and Calmodulin (CMDN)

Buffered $[TRPN]=[\overline{TRPN}]\{[Ca^{2+}]_i/([Ca^{2+}]_i+K_{m,TRPN})\}$

Buffered $[CMDN]=[\overline{CMDN}]\{[Ca^{2+}]_i/([Ca^{2+}]_i+K_{m,CMDN})\}$

$[\overline{TRPN}]=70\ \mu$mol/L

$[\overline{CMDN}]=50\ \mu$mol/L

$K_{m,TRPN}=0.5\ \mu$mol/L

$K_{m,CMDN}=2.38\ \mu$mol/L

where $K_{m,TRPN}$ is the half-saturation concentration of TRPN, and $K_{m,CMDN}$ is the half-saturation concentration of CMDN.

Ca^{2+} Buffer in JSR: Calsequestrin (CSQN)

Buffered$[CSQN]=[\overline{CSQN}]\{[Ca^{2+}]_{JSR}/([Ca^{2+}]_{JSR}+K_{m,CSQN})\}$

$[\overline{CSQN}]=10$ mmol/L

$K_{m,CSQN}=0.8$ mmol/L

where $K_{m,CSQN}$ is the half-saturation concentration of CSQN.

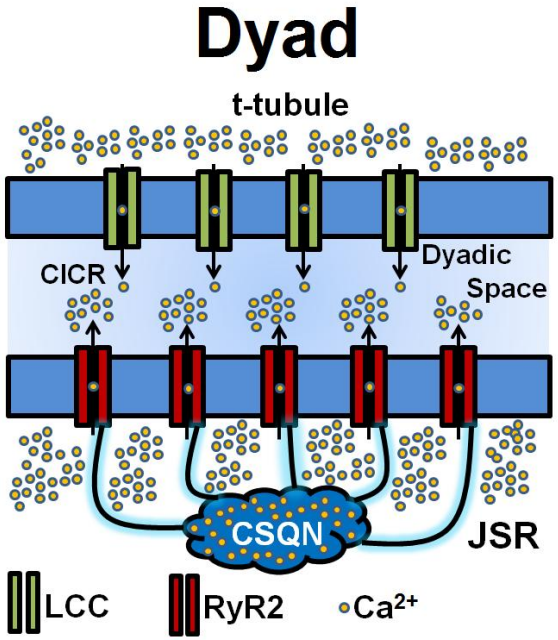

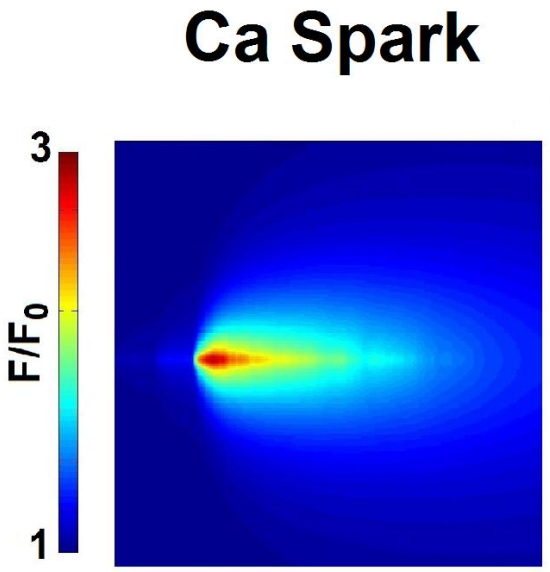

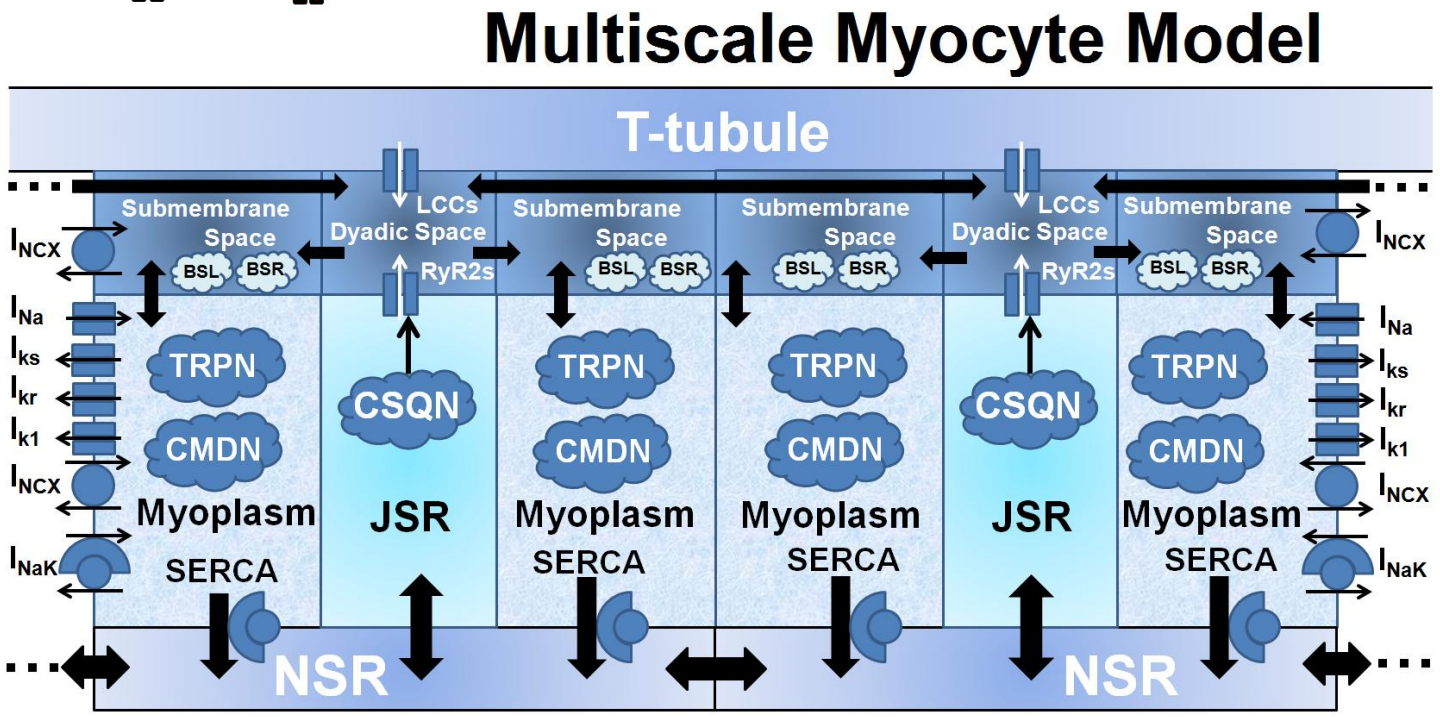

Gaur&Rudy, Biophys J 2011, 100 (12): 2904-12.

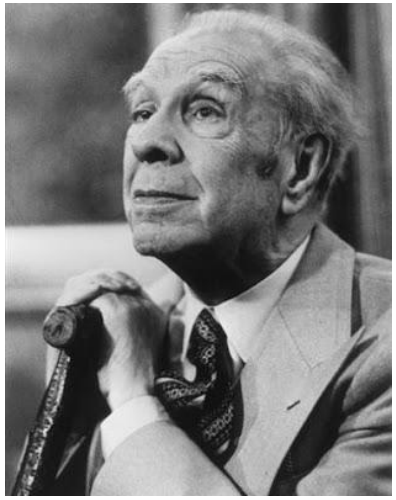

DEL RIGORE NELLA SCIENZA

... In quell'Impero, l'Arte della Cartografia raggiunse tale Perfezione che la mappa di una sola Provincia occupava un'intera Città, e la mappa dell'Impero un'intera Provincia. Col tempo, queste Mappe Smisurate non soddisfecero più e i Collegi dei **Cartografi crearono una Mappa dell'Impero che aveva la grandezza stessa dell'Impero e con esso coincideva esattamente.** Meno Dedite allo Studio della Cartografia, le Generazioni Successive capirono che **quella immensa Mappa era Inutile** e non senza Empietà l'abbandonarono alle Inclemenze del Sole e degli Inverni. Nei deserti dell'Ovest restano ancora lacere Rovine della Mappa, abitate da Animali e Mendicanti; nell'intero Paese non vi sono altre reliquie delle Discipline Geografiche.

Da **Jorge Luis Borges** , *L'artefice*

Modello di FitzHugh-Nagumo

$$\begin{cases} \dfrac{dV}{dt} = g(V) - W + I_a \\ \dfrac{dW}{dt} = bV - hW \end{cases}$$

$$\begin{cases} \dfrac{\partial V}{\partial t} = \dfrac{1}{\epsilon}(V - V^3/3 - W) \\ \dfrac{\partial W}{\partial t} = \epsilon(V - \gamma W + \beta) \end{cases}$$

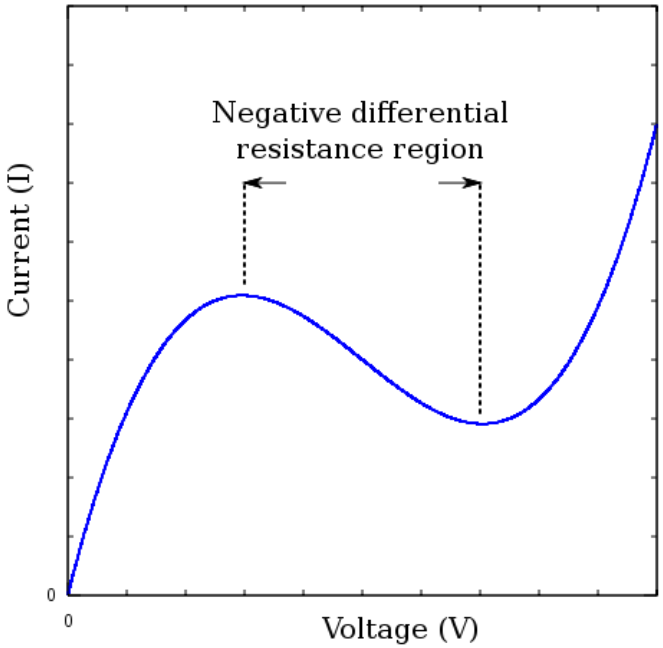

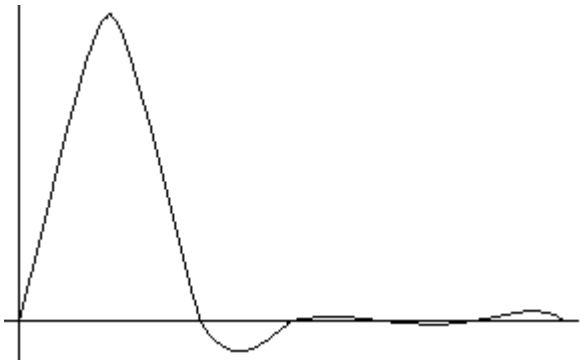

Propagazione del POTENZIALE D'AZIONE CARDIACO attraverso le **GAP JUNCTIONS**

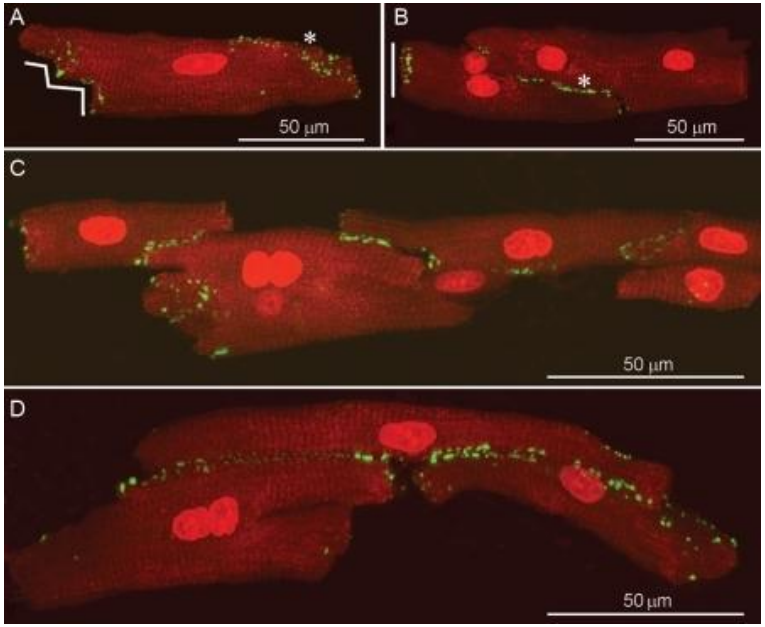

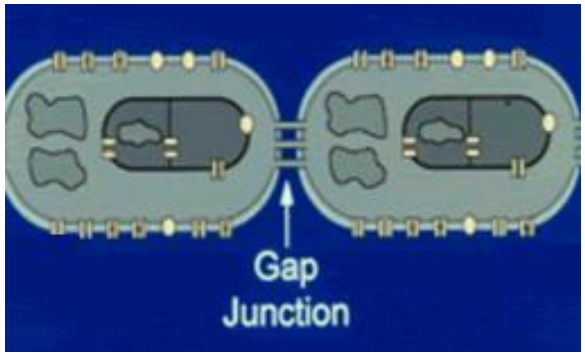

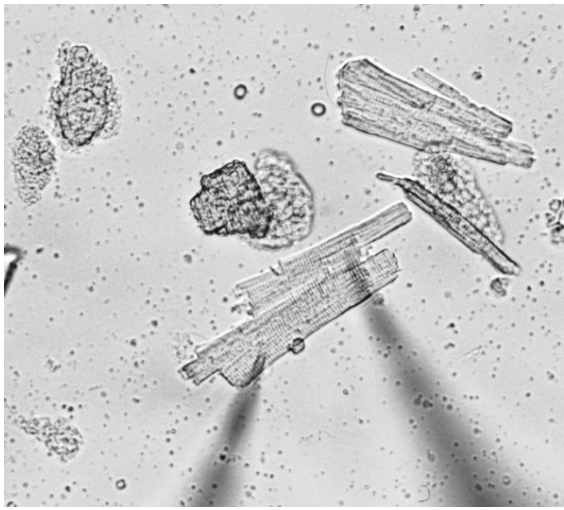

tecnica del
DOUBLE-PATCH CLAMP

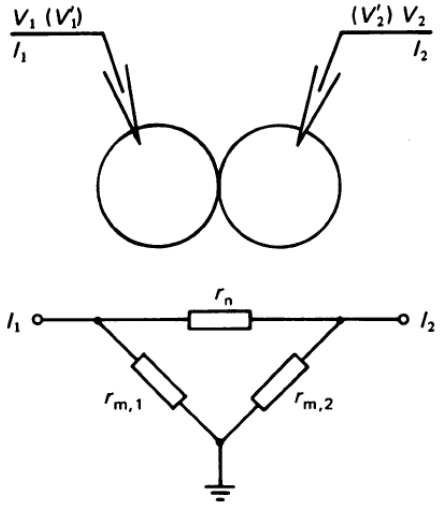

$$\begin{cases} \dfrac{dV_1}{dI_1} = \dfrac{r_{m,1}(r_{m,2}+r_n)}{r_{m,1}+r_{m,2}+r_n}, \\ \dfrac{dV_2'}{dV_1} = \dfrac{r_{m,2}}{r_{m,2}+r_n}. \end{cases}$$

$r_n = 2 – 10\ M\Omega$

Zaniboni et al. *Circ Res* 2003, vol. 93, p. 726-735

Tecnica del **COUPLING CLAMP**

"in vivo"

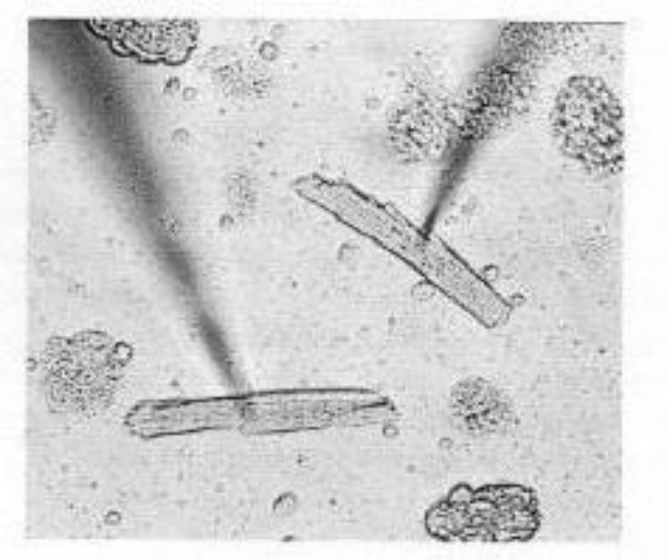

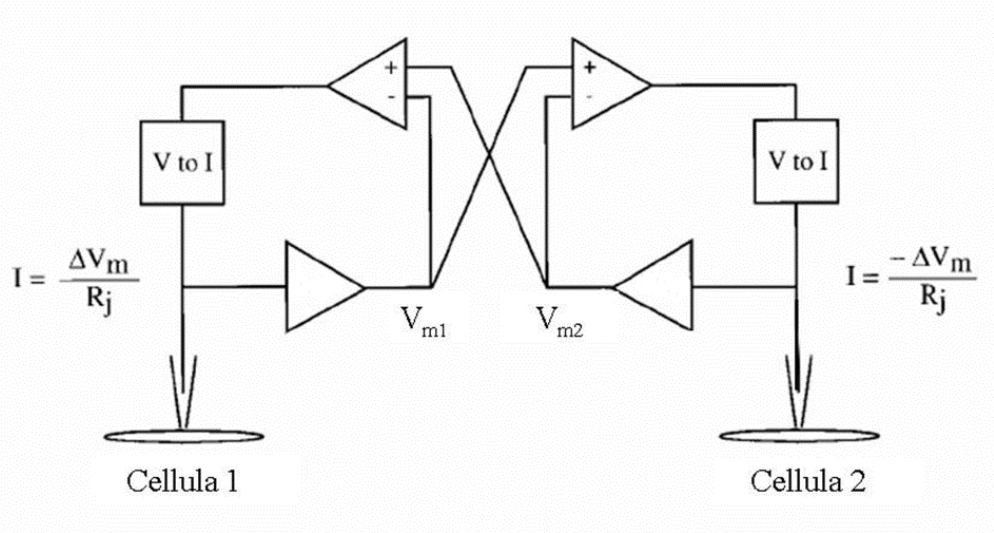

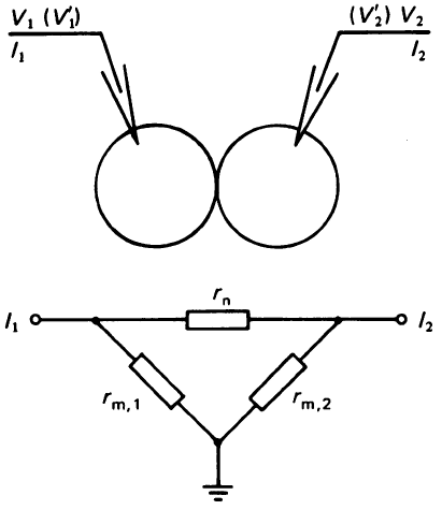

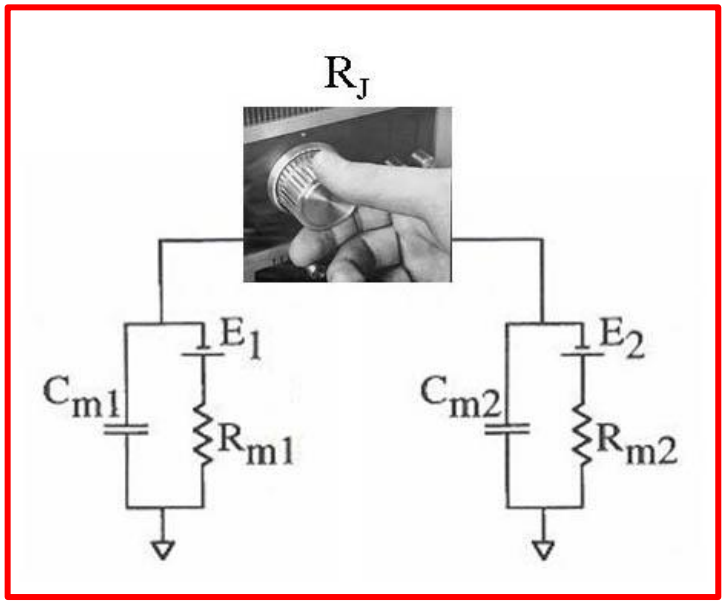

Zaniboni et al. *Am J Physiol* 2000, vol. 278, p. 677-687

aumento del ritardo *nella conduzione* *"in vivo"*

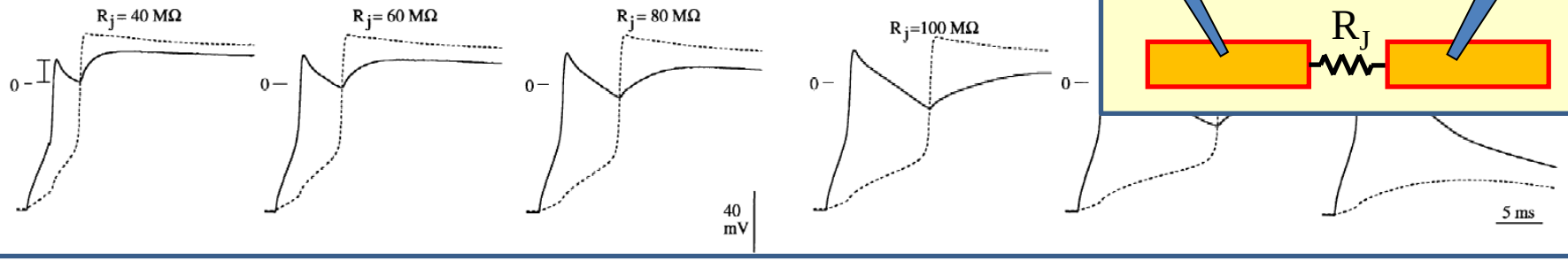

sincronizzazione della ripolarizzazione

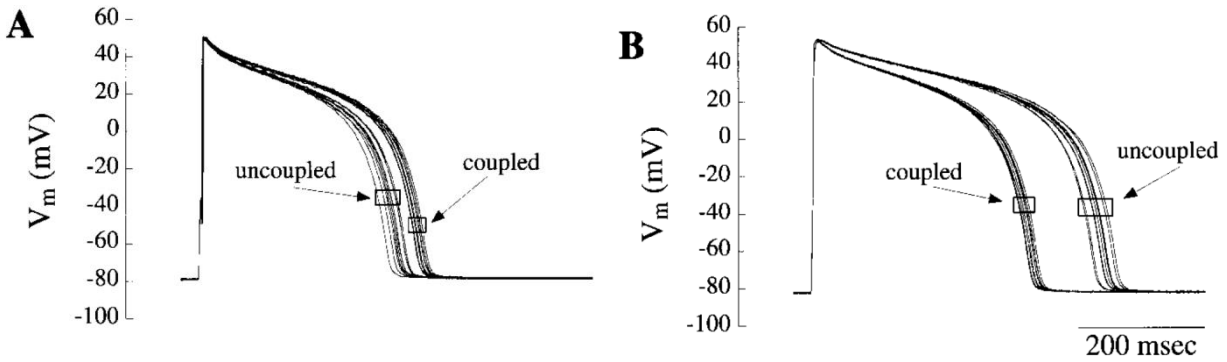

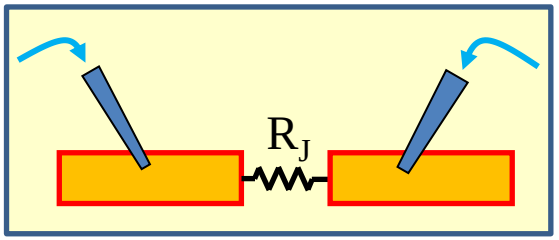

sincronizzazione del battito

$R_J = \infty$

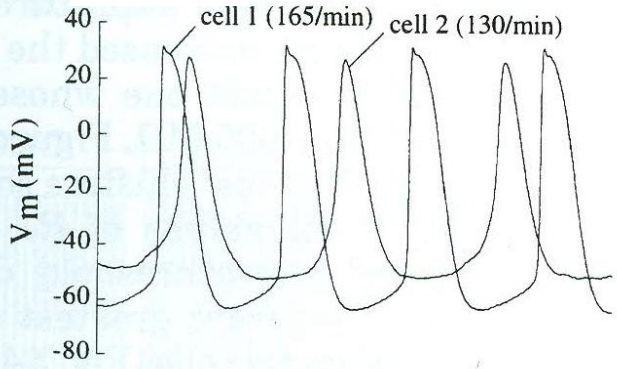

$R_J = 500\ M\Omega$

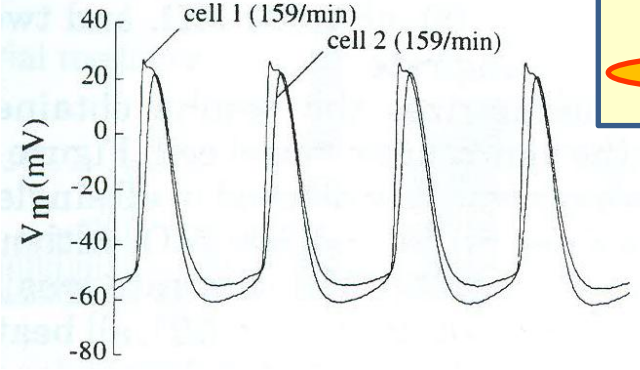

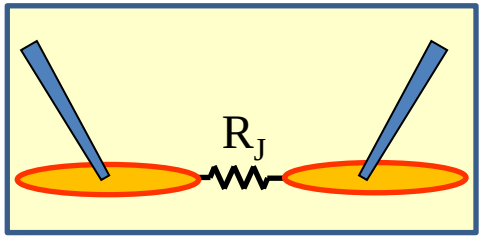

"in silico"

$$\begin{cases} C\dfrac{dV_1}{dt} = I_{ion1} + I_{et} \\ \dfrac{dm_1}{dt} = \ldots \\ \ldots\ldots \\ \ldots\ldots \end{cases}$$

$$I_{et} = \frac{(V_1 - V_2)}{R_J}$$

$$\begin{cases} C\dfrac{dV_2}{dt} = I_{ion2} - I_{et} \\ \dfrac{dm_2}{dt} = \ldots \\ \ldots\ldots \\ \ldots\ldots \end{cases}$$

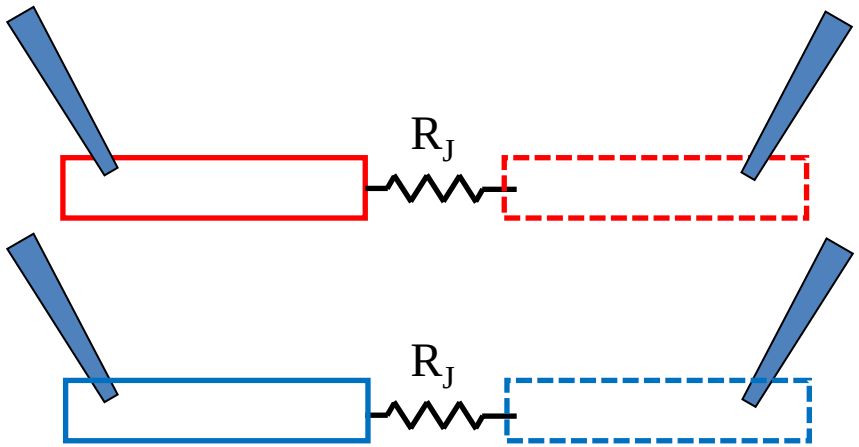

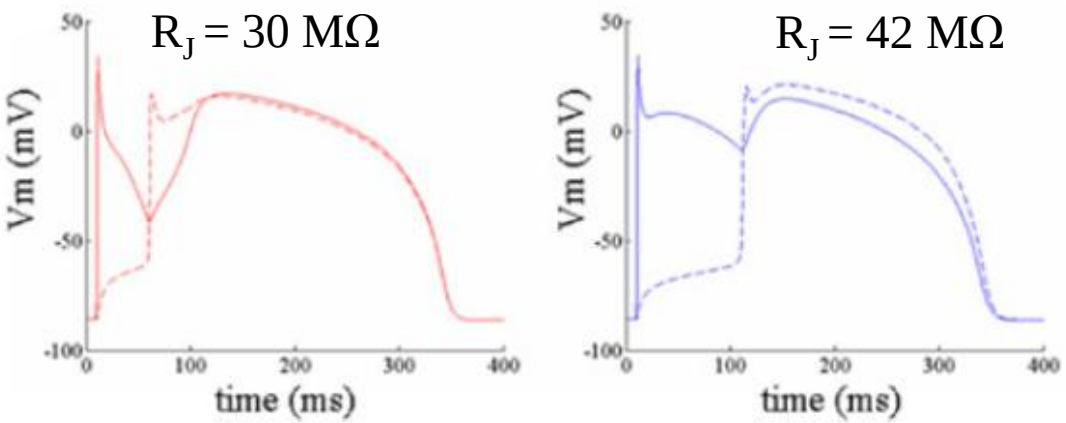

Zaniboni et al. *Math Biosci* 2011, vol. 228, p. 56-70

EQUAZIONE DEL CAVO

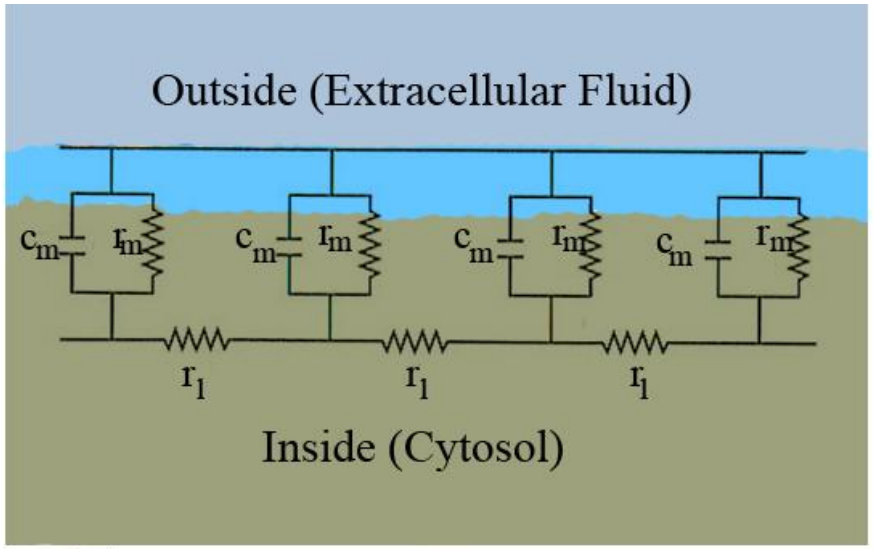

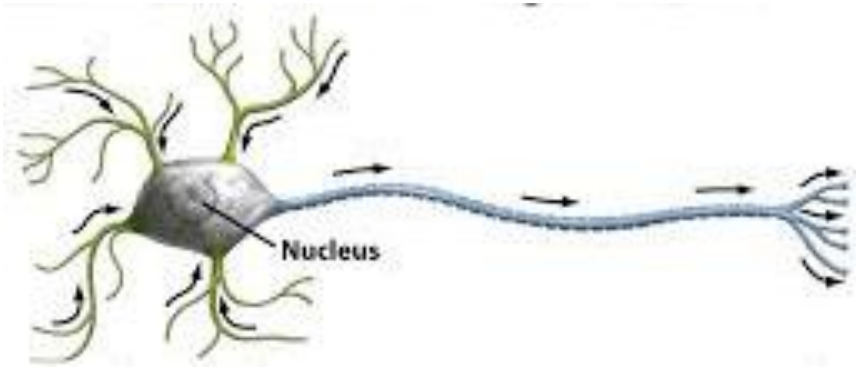

r_m: Membrane resistance
r_l : Longitudinal resistance
c_m: Capacitance due to electrostatic forces

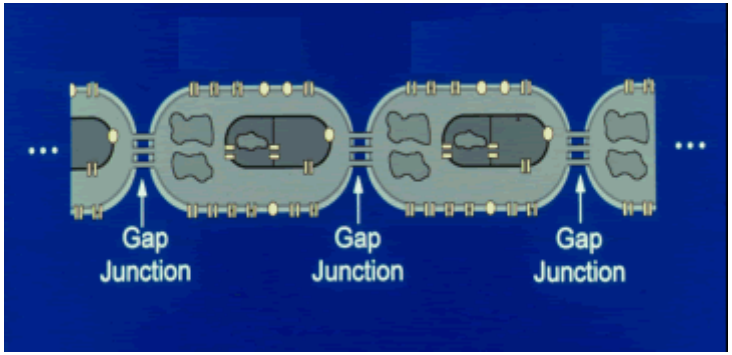

$$\frac{1}{r_l}\frac{\partial^2 V}{\partial x^2} = c_m \frac{\partial V}{\partial t} + \frac{V}{r_m}$$

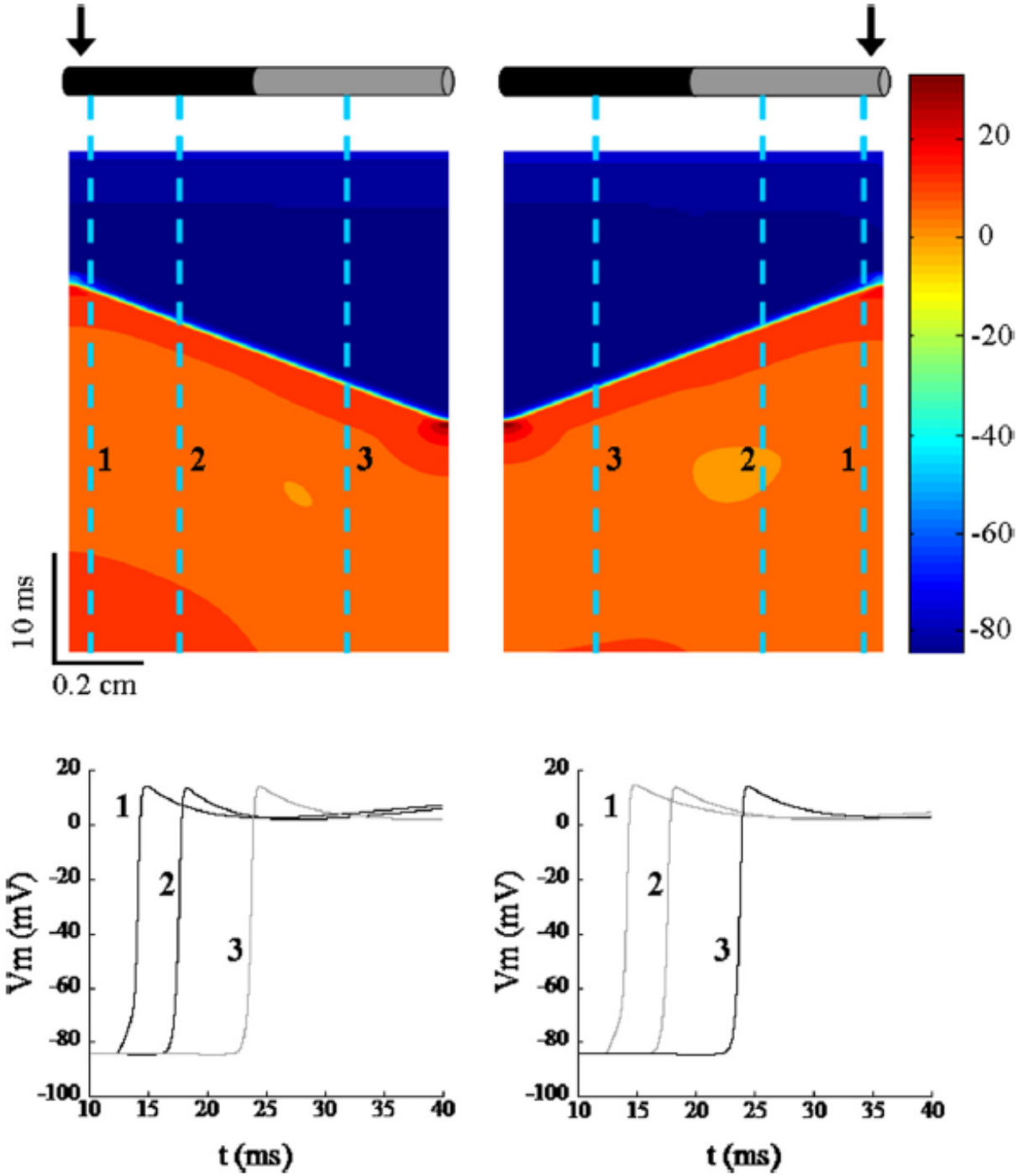
1
2
3
3
2
1
20
0
-20
-40
-60
-80
10 ms
0.2 cm
Vm (mV)
t (ms)
Vm (mV)
t (ms)

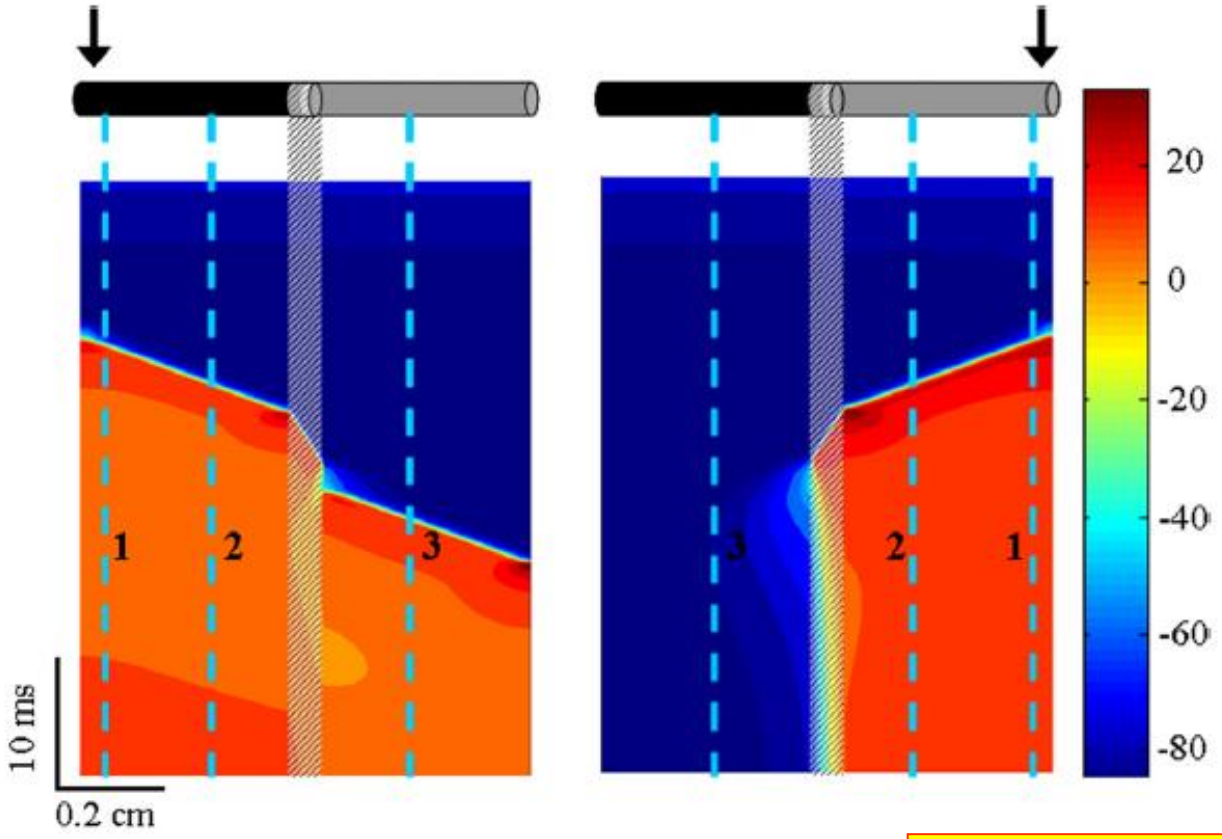

BLOCCO UNIDIRETTIVO

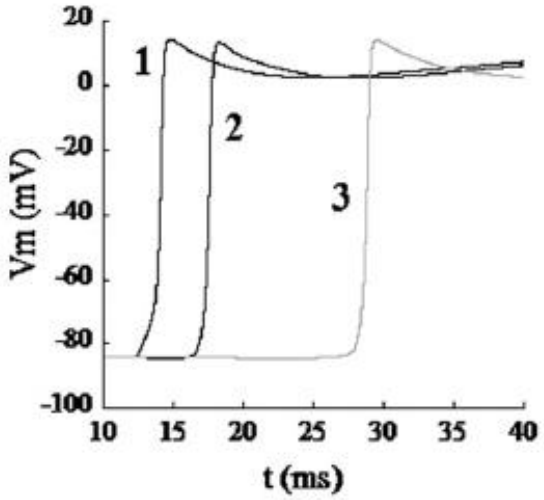

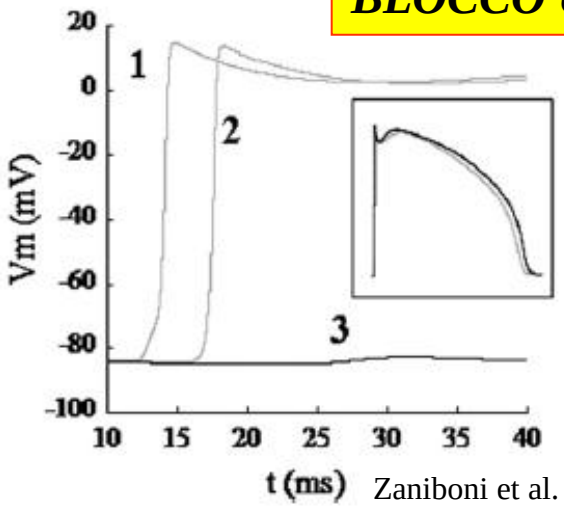

Zaniboni et al. *Math Biosci* 2010, vol. 228, p. 56-70

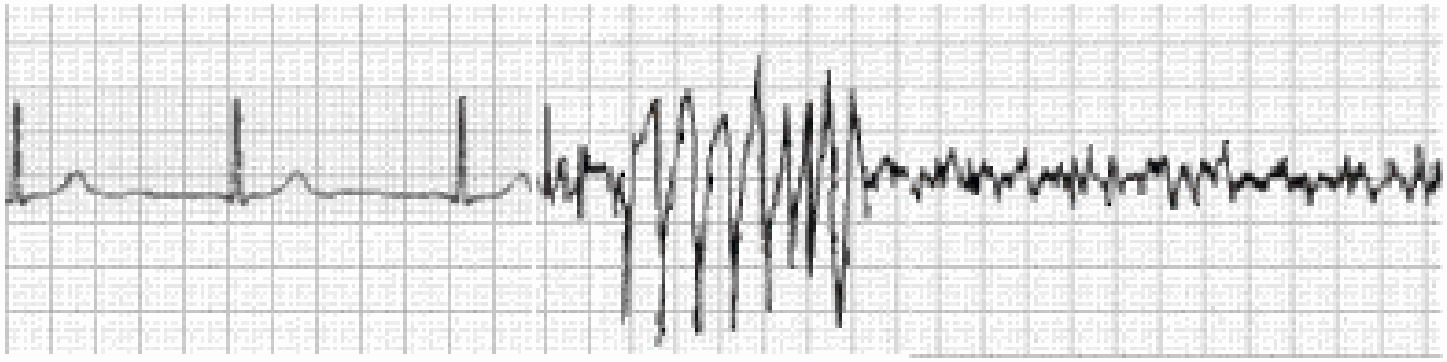

Normal Heart Rhythm

Ventricular Tachycardia

Ventricular Fibrillation

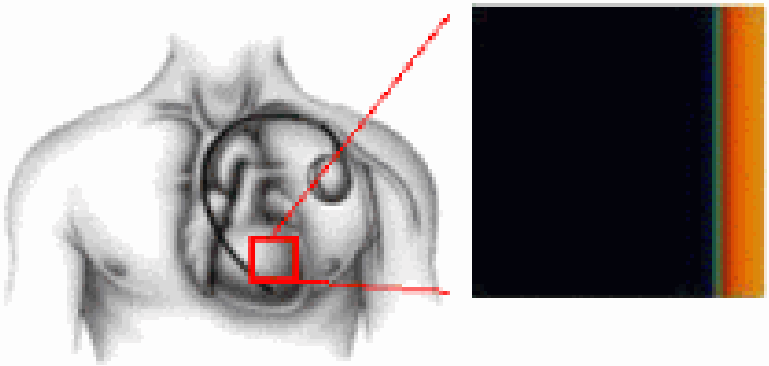

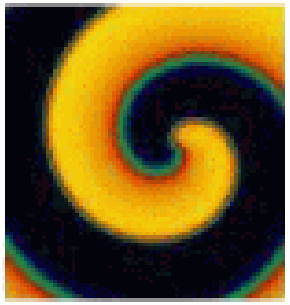

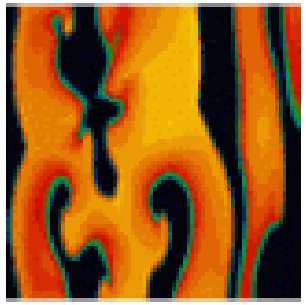

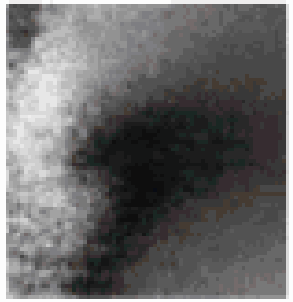

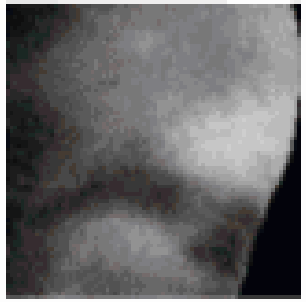

Simulation

-85 mV 20 mV

Experiment

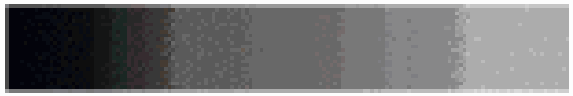

-85 mV 20 mV

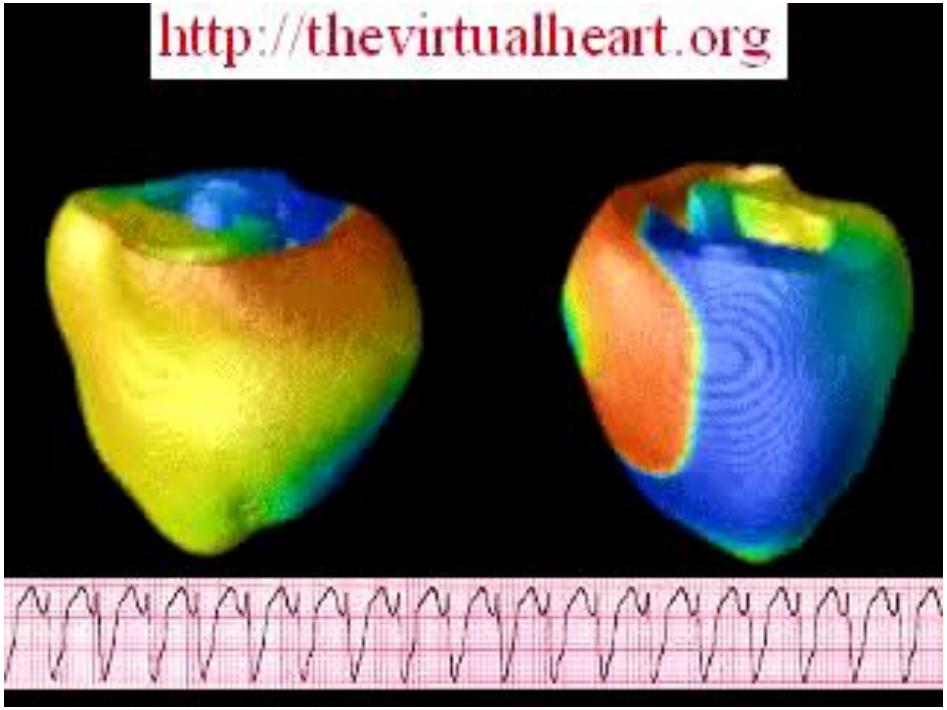

ONDE SPIRALI DI PROPAGAZIONE di potenziali d'azione tipo **Fitzhugh-Nagumo**

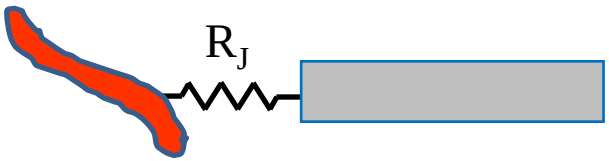
R_J

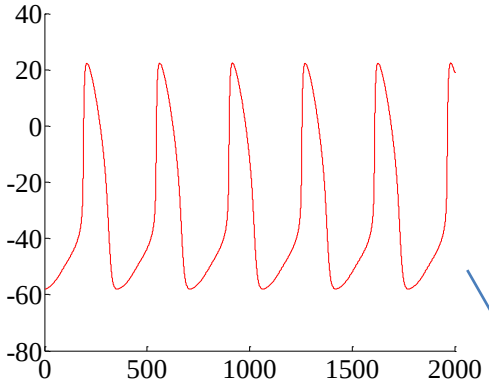
40
20
0
-20
-40
-60
-80
0
500
1000
1500
2000

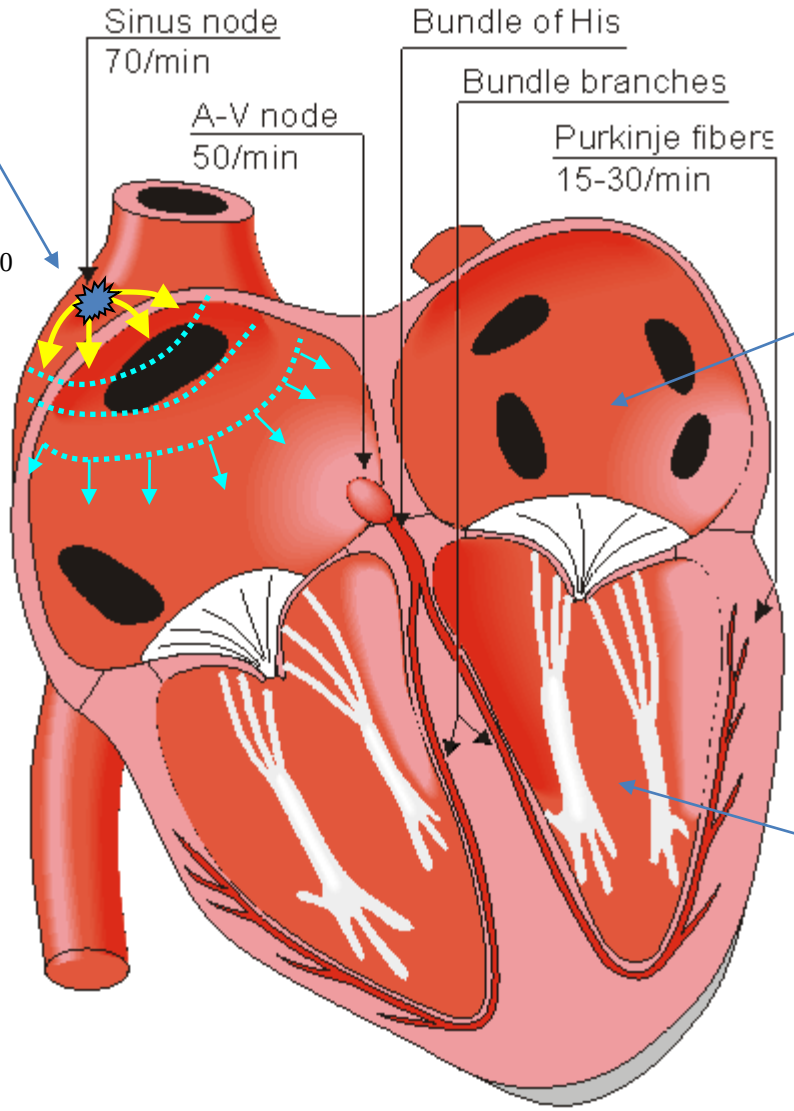
Sinus node
70/min
A-V node
50/min
Bundle of His
Bundle branches
Purkinje fibers
15-30/min

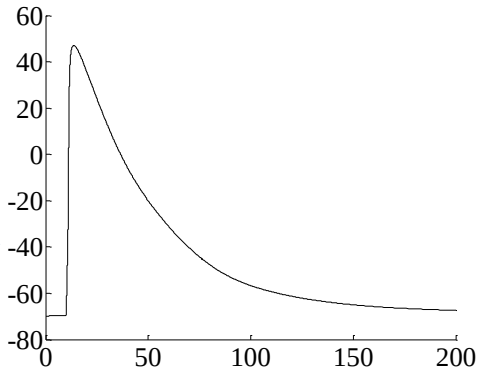
60
40
20
0
-20
-40
-60
-80
0
50
100
150
200

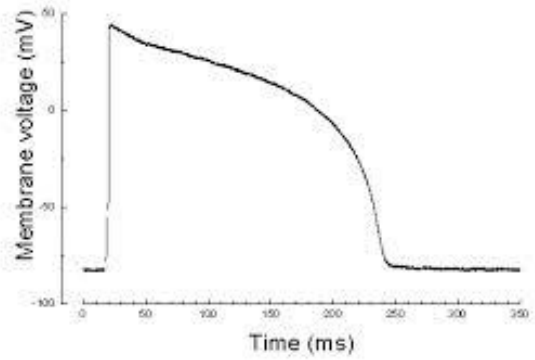
Membrane voltage (mV)
Time (ms)

"in silico"

$$\begin{cases} C\dfrac{dV_1}{dt} = I_{ion1} + I_{et} \\ \dfrac{dm_1}{dt} = \ldots \\ \ldots\ldots \\ \ldots\ldots \end{cases}$$

$$I_{et} = \frac{(V_1 - V_2)}{R_J}$$

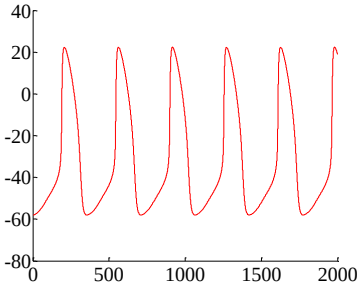

modello AP cellula pacemaker

$$\begin{cases} C\dfrac{dV_2}{dt} = I_{ion2} - I_{et} \\ \dfrac{dm_2}{dt} = \ldots \\ \ldots\ldots \\ \ldots\ldots \end{cases}$$

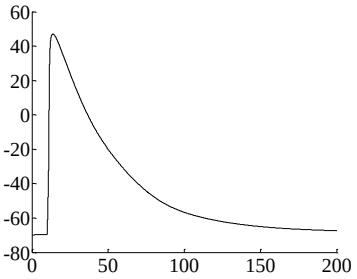

modello AP cellula atriale

CANALE DI
GAP JUNCTION

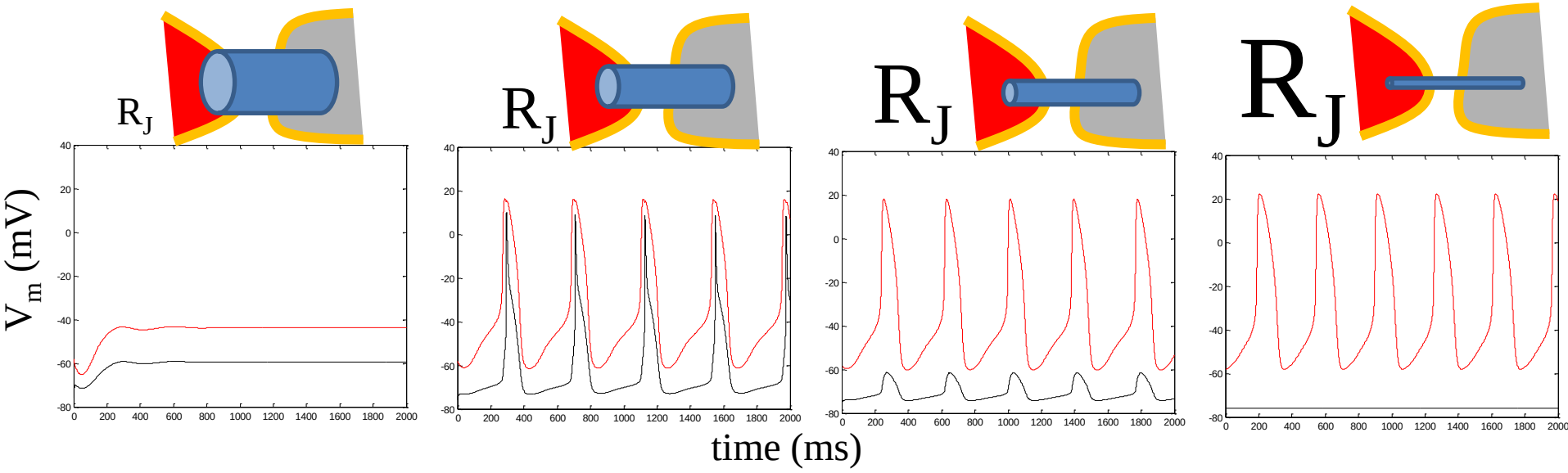

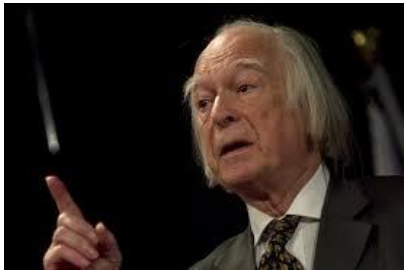

Denis Noble

SA nodal
atrial
gap junctions low resistance
gap junctions high resistance

Role of junctional coupling in pacemaker potential conduction

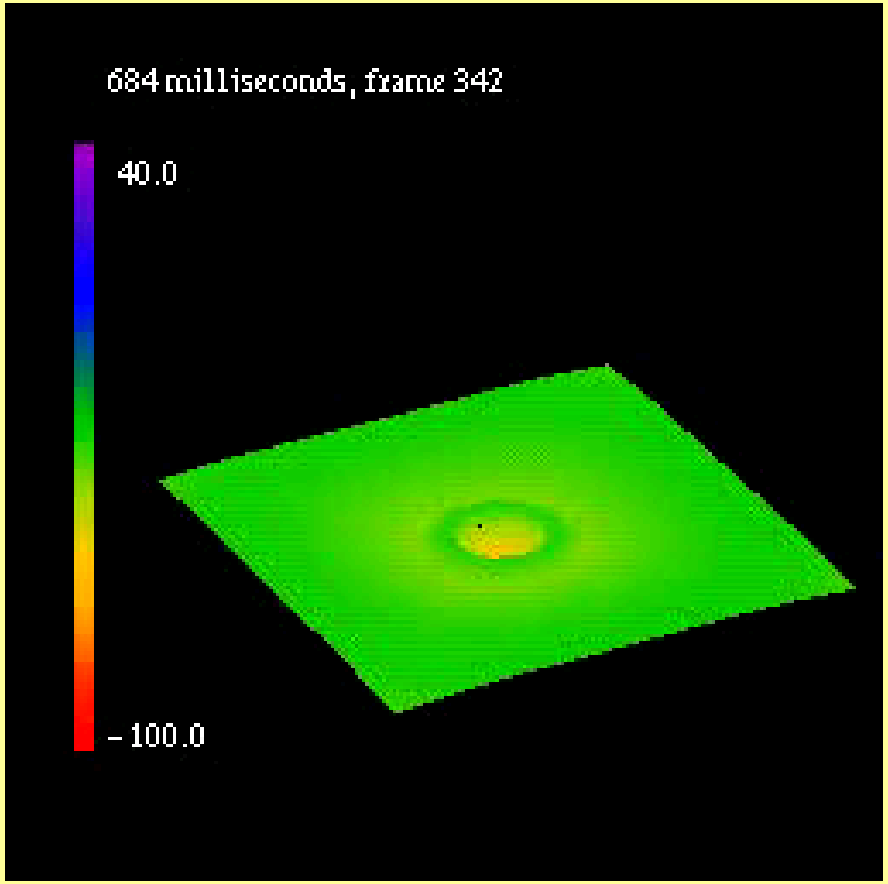

This animation shows a computer model of a pacemaking SA node embedded in surrounding atrial tissue. Individual SA node cells are based on the model of Cai, Winslow, and Noble (IEEE Trans. BME. 41(3):217-231). Atrial cells are modeled as described in Winslow et al. (Proc. Roy. Soc. Lond. B, 254: 55-61). Cell-to-cell coupling in the SA node is 10 nS, and is 50 nS in the surrounding atrium. Coupling at the border between SA node and atrium is 50 nS. At this level of coupling, the pacemaking node is able to generate a propagating wave of excitation in the atrium.

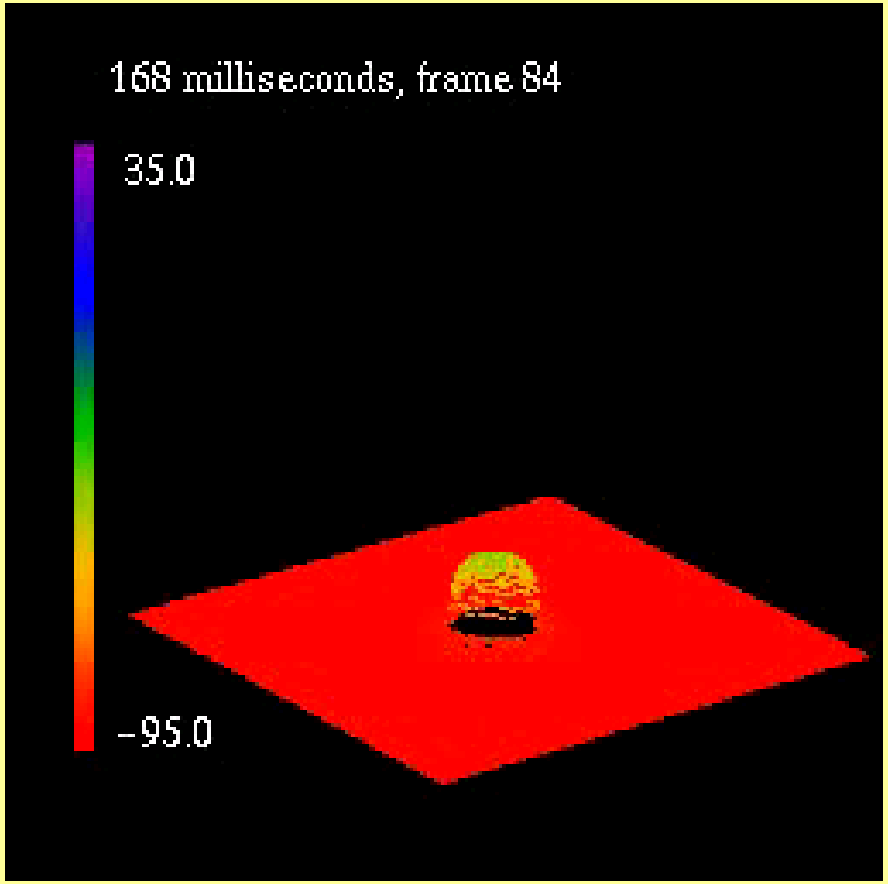

In this animation, cell-to-cell coupling within the atrium and at the SA node - atrial border is increased from 50 to 100 nS. This coupling level is so high that electrotonic loading of peripheral SA node cells by surrounding atrial cells prevents them from oscillating, and the pacemaker potential fails to conduct onto the atrium. Electrotonic loading occurs since atrial cells have a resting potential (roughly -90 mV) which is considerably more hyperpolarized than the maximum diastolic potential of peripheral SA node cells (-70 mV).

*Evidenze sperimentali di un **GRADIENTE nella distribuzione delle GJ** nel Nodo Senoatriale*

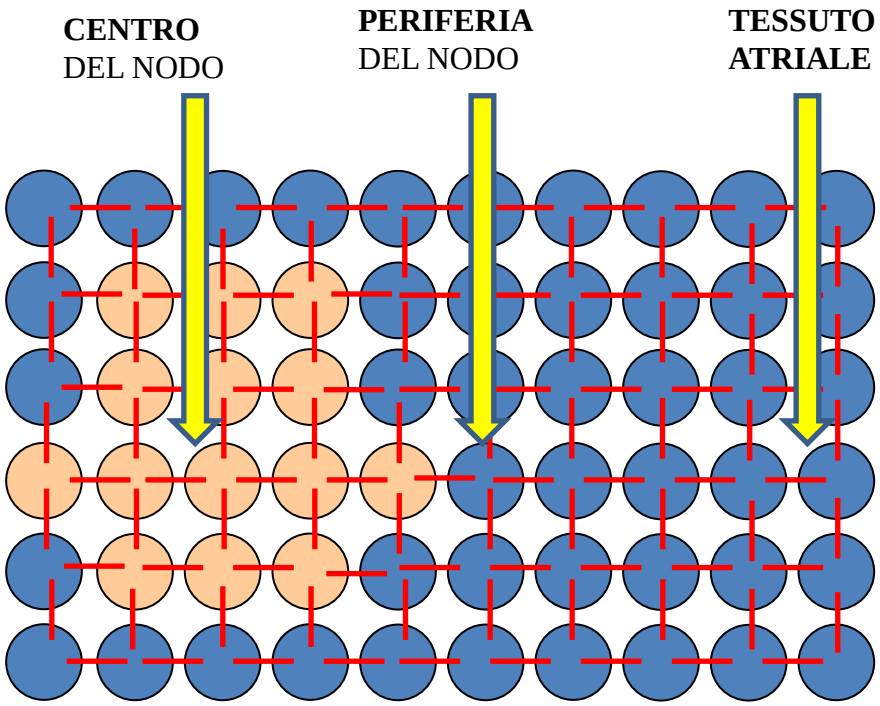

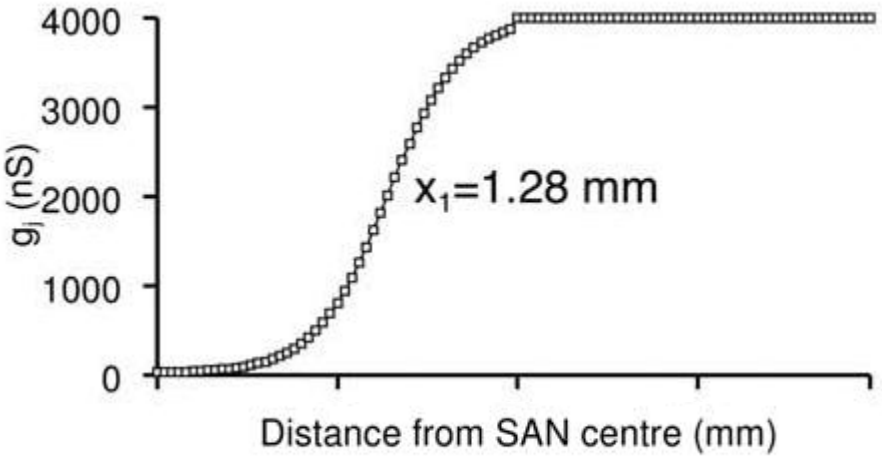

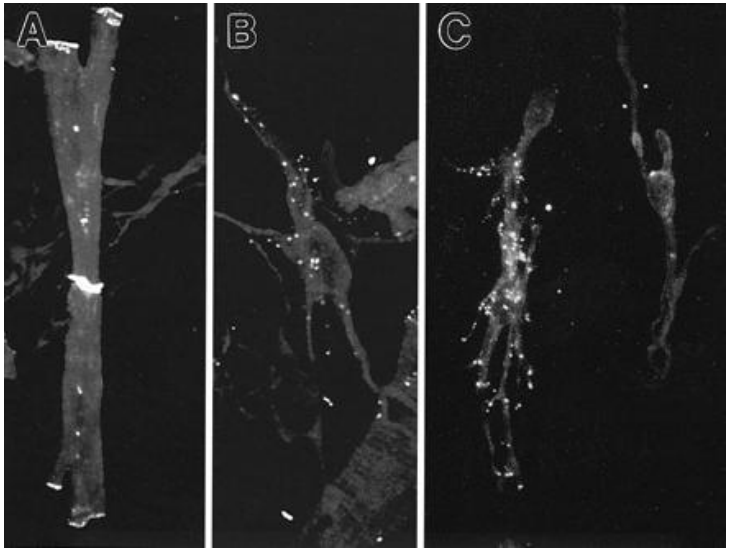

Inada et al., *Importance of gradients in membrane properties and electrical coupling in sinoatrial node pacing.* PloS One 2014;9(4):e94565

Le frontiere …

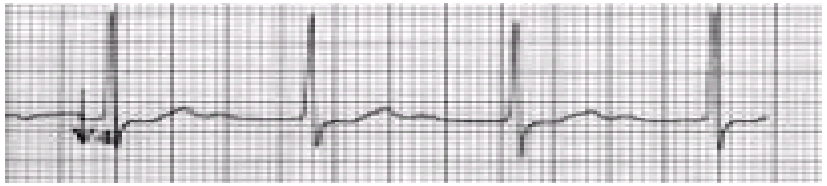

Moderna registrazione di ECG

Bruno Taccardi, Università di Parma
Emilio Gatti, Politecnico di Milano
Piero Colli-Franzone, Università di Pavia

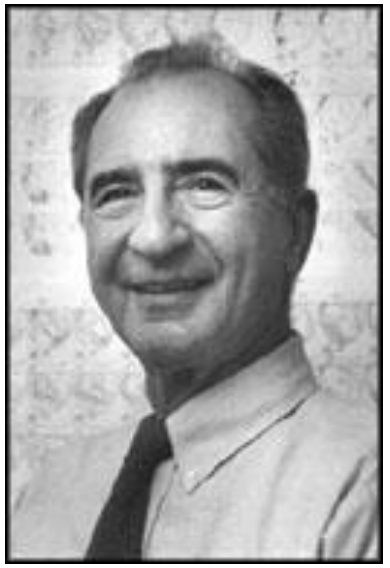

Prof. Bruno Taccardi

TACCARDI B. Circ Res. 1963; 12: 341-52.
Distribution of heart potentials on the thoracic surface of normal human subjects.

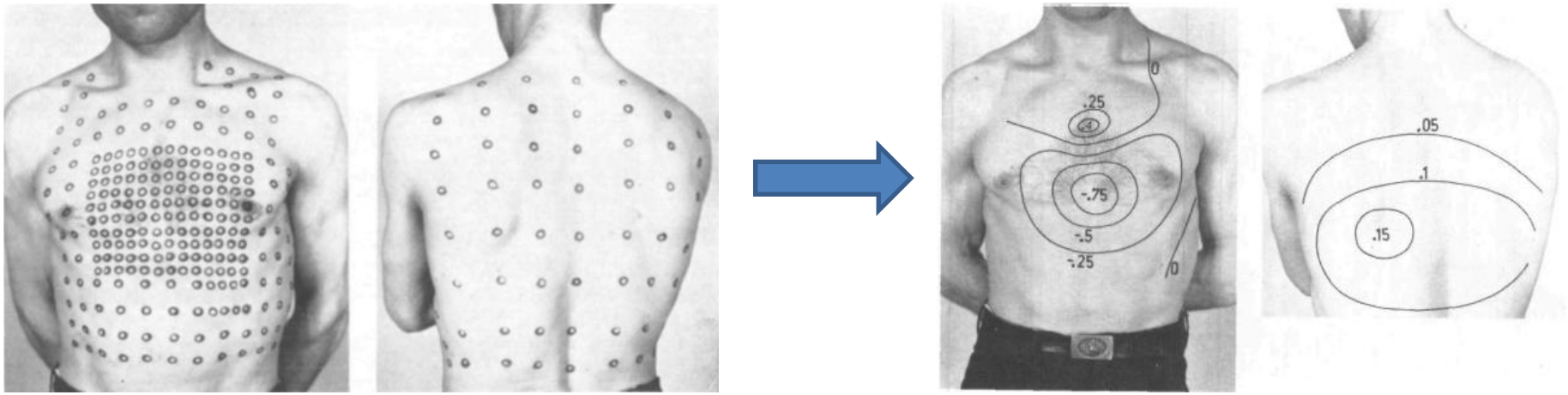

BODY SURFACE MAPPING

SURFACE POTENTIAL MAPPING

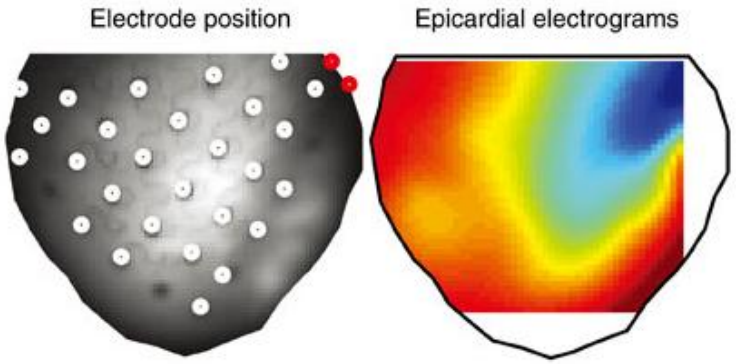

PROBLEMA INVERSO

"È possibile ricostruire la mappa dei potenziali epicardici a partire da quella dei potenziali di torso?"

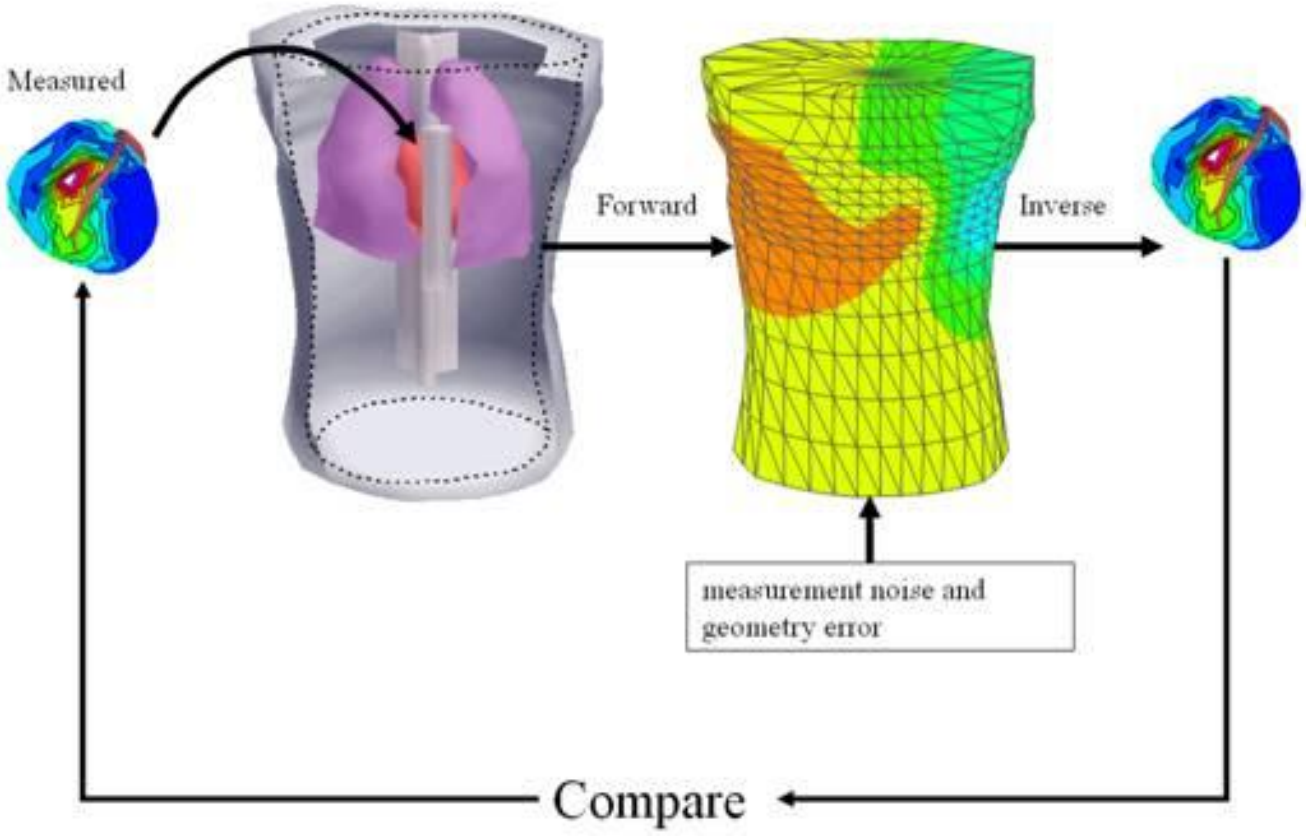

Yoram Rudy, Washington University in St. Louis

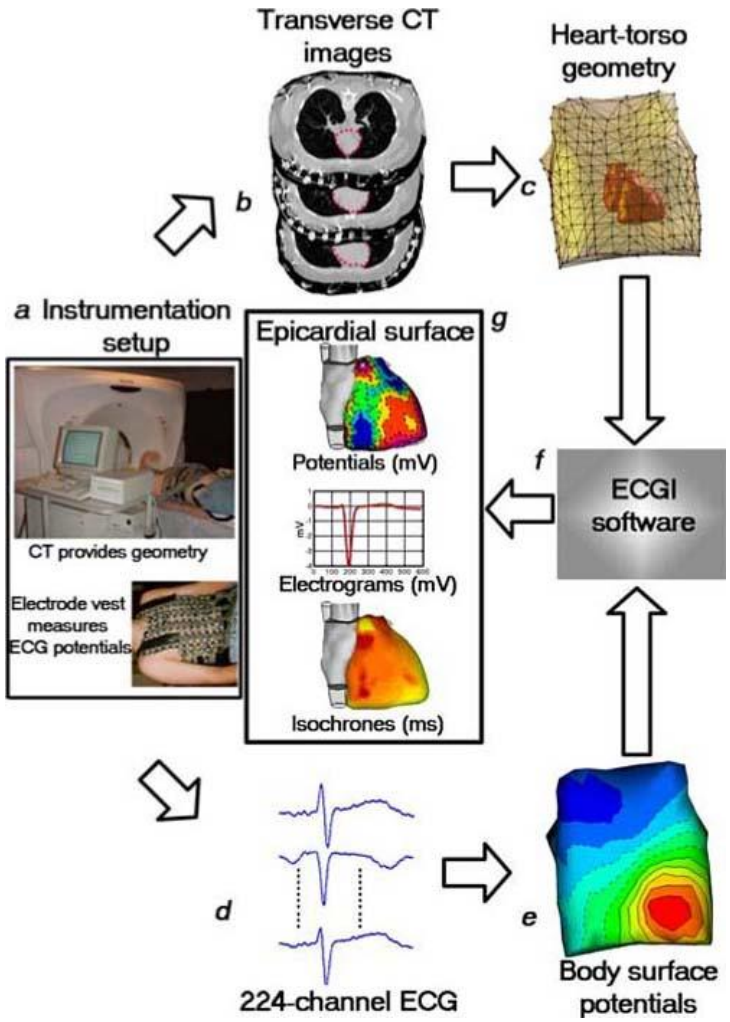

2014

… forte e misterioso regolatore della nostra vita e obbediente a leggi più complicate delle nostre, è quell'astro rosso che palpita nel buio del nostro corpo, sospeso nella sua gabbia d'ossa e di carne.

M. Yourcenar, *L'opera al nero*

GRAZIE PER L'ATTENZIONE